AD-A168 114 A DOUBLY ASYMPTOTIC NON-REFLECTING BOUNDARY FOR GROUND-SHOCK ANALYSIS (U) LOCKHEED MISSILES AND SPACE CO INC PALO ALTO CA I C MATHEWS ET AL. 31 JAN 85 1/1

UNCLASSIFIED LMSC-F035826 DNA-TR-85-244 DNA001-83-C-0239 F/G 13/13 NL

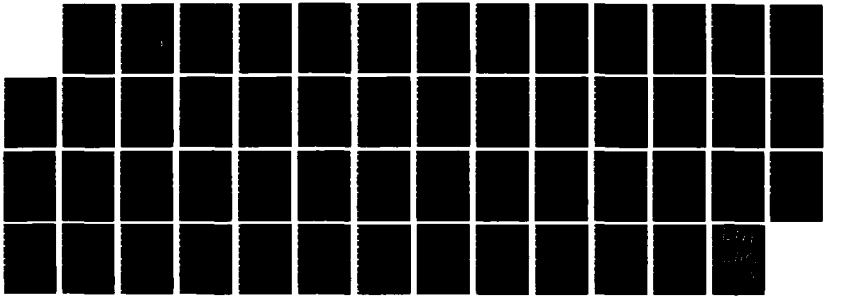

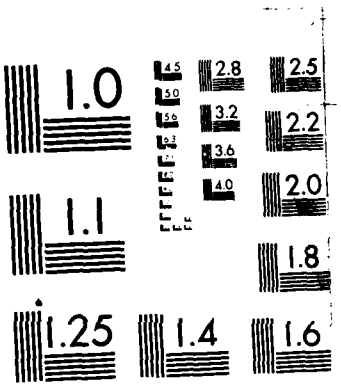

DNA-TR-85-244

# A DOUBLY ASYMPTOTIC, NON-REFLECTING BOUNDARY FOR GROUND-SHOCK ANALYSIS

Ian C. Mathews
Thomas L. Geers
Lockheed Missiles & Space Co., Inc.
3251 Hanover Street
Palo Alto, CA 94306-1245

31 January 1985

Technical Report

CONTRACT No. DNA 001-83-C-0239



Approved for public release; distribution is unlimited.

THIS WORK WAS SPONSORED BY THE DEFENSE NUCLEAR AGENCY UNDER RDT&E RMSS CODE B344083466 Y99QAXSC00067 H2590D.



Prepared for
Director
DEFENSE NUCLEAR AGENCY
Washington, DC 20305-1000

Destroy this report when it is no longer needed. Do not return to sender.

PLEASE NOTIFY THE DEFENSE NUCLEAR AGENCY, ATTN: STTI, WASHINGTON, DC 20305-1000, IF YOUR ADDRESS IS INCORRECT, IF YOU WISH IT DELETED FROM THE DISTRIBUTION LIST, OR IF THE ADDRESSEE IS NO LONGER EMPLOYED BY YOUR ORGANIZATION.

# DISTRIBUTION LIST UPDATE

This mailer is provided to enable DNA to maintain current distribution lists for reports. We would appreciate your providing the requested information.

☐ Add the individual listed to your distribution list.

☐ Delete the cited organization/individual.

☐ Change of address.

NAME: _____

ORGANIZATION: _____

| OLD ADDRESS | CURRENT ADDRESS |
|---|---|
| _____ | _____ |
| _____ | _____ |
| _____ | _____ |

TELEPHONE NUMBER: (  ) _____

SUBJECT AREA(s) OF INTEREST:

| | |
|---|---|
| _____ | _____ |
| _____ | _____ |
| _____ | _____ |

DNA OR OTHER GOVERNMENT CONTRACT NUMBER: _____

CERTIFICATION OF NEED-TO-KNOW BY GOVERNMENT SPONSOR (if other than DNA):

SPONSORING ORGANIZATION: _____

CONTRACTING OFFICER OR REPRESENTATIVE: _____

SIGNATURE: _____

Director
Defense Nuclear Agency
ATTN: STTI
Washington, DC 20305-1000

Director
Defense Nuclear Agency
ATTN: STTI
Washington, DC 20305-1000

UNCLASSIFIED
SECURITY CLASSIFICATION OF THIS PAGE

AD-A168 114

# REPORT DOCUMENTATION PAGE

Form Approved
OMB No. 0704-0188
Exp. Date: Jun 30, 1986

| | |
|---|---|
| 1a. REPORT SECURITY CLASSIFICATION<br>UNCLASSIFIED | 1b. RESTRICTIVE MARKINGS |
| 2a. SECURITY CLASSIFICATION AUTHORITY<br>N/A since Unclassified | 3. DISTRIBUTION/AVAILABILITY OF REPORT<br>Approved for public release; distribution is unlimited. |
| 2b. DECLASSIFICATION/DOWNGRADING SCHEDULE<br>N/A since Unclassified | |
| 4. PERFORMING ORGANIZATION REPORT NUMBER(S)<br>LMSC-F035826 | 5. MONITORING ORGANIZATION REPORT NUMBER(S)<br>DNA-TR-85-244 |
| 6a. NAME OF PERFORMING ORGANIZATION<br>Lockheed Missiles and Space Co, Inc.<br>6b. OFFICE SYMBOL (If applicable) | 7a. NAME OF MONITORING ORGANIZATION<br>Director<br>Defense Nuclear Agency |
| 6c. ADDRESS (City, State, and ZIP Code)<br>3251 Hanover Street<br>Palo Alto, CA 94306-1245 | 7b. ADDRESS (City, State, and ZIP Code)<br>Washington, DC 20305-1000 |
| 8a. NAME OF FUNDING/SPONSORING ORGANIZATION<br>8b. OFFICE SYMBOL (If applicable) | 9. PROCUREMENT INSTRUMENT IDENTIFICATION NUMBER<br>DNA 001-83-C-0239 |
| 8c. ADDRESS (City, State, and ZIP Code) | 10. SOURCE OF FUNDING NUMBERS |

| PROGRAM ELEMENT NO. | PROJECT NO | TASK NO. | WORK UNIT ACCESSION NO. |
|---|---|---|---|
| 62715H | Y99QAXS | C | DH006841 |

11. TITLE (Include Security Classification)
A DOUBLY ASYMPTOTIC, NON-REFLECTING BOUNDARY FOR GROUND-SHOCK ANALYSIS

12. PERSONAL AUTHOR(S)
Mathews, Ian C. and Geers, Thomas L.

| 13a. TYPE OF REPORT | 13b. TIME COVERED | 14. DATE OF REPORT (Year, Month, Day) | 15. PAGE COUNT |
|---|---|---|---|
| Technical Report | FROM 830801 TO 850130 | 850131 | 50 |

16. SUPPLEMENTARY NOTATION
This work was sponsored by the Defense Nuclear Agency under RDT&E RMSS Code B344083466 Y99QAXSC00067 H2590D.

| 17 COSATI CODES | | | 18. SUBJECT TERMS (Continue on reverse if necessary and identify by block number) |
|---|---|---|---|
| FIELD | GROUP | SUB-GROUP | |
| 12 | 1 | | Ground Shock, Elastrodynamics Scattering, |
| 20 | 11 | | Finite Elements, Doubly Asymptotic Approximations, sub 1 |
| | | | Boundary Elements, |

19. ABSTRACT (Continue on reverse if necessary and identify by block number)

This report describes the formulation and implementation of a nonreflecting boundary for use with existing finite-element codes to perform nonlinear ground-shock analyses of buried structures. The boundary is based on a first-order doubly asymptotic approximations (DAA) for disturbances propagating outward from a selected portion of the soil medium surrounding the structure of interest. The resulting set of first-order ordinary differential equations is then combined with the second-order equations of motion for the finite-element model so as to facilitate solution by a staggered solution procedure. This procedure is shown to be computationally stable as long as the time increment is smaller than a limiting value based on the finite-element mass matrix and the DAA-boundary stiffness matrix. Computational results produced by the boundary are compared with exact results for linear, canonical problems pertaining to infinite-cylindrical and spherical shells.

| 20. DISTRIBUTION/AVAILABILITY OF ABSTRACT | 21. ABSTRACT SECURITY CLASSIFICATION |
|---|---|
| ☐ UNCLASSIFIED/UNLIMITED ☒ SAME AS RPT ☐ DTIC USERS | UNCLASSIFIED |
| 22a. NAME OF RESPONSIBLE INDIVIDUAL<br>Betty L. Fox | 22b. TELEPHONE (Include Area Code)<br>(202) 325-7042 |
| | 22c. OFFICE SYMBOL<br>DNA/STTI |

DD FORM 1473, 84 MAR 83 APR edition may be used until exhausted
All other editions are obsolete

SECURITY CLASSIFICATION OF THIS PAGE
UNCLASSIFIED

## SUMMARY

This report describes the formulation and implementation of a *nonreflecting boundary* for use with existing finite-element codes to perform nonlinear ground-shock analyses of buried structures. The boundary is based on a first-order *doubly asymptotic approximation* ($DAA_1$) for disturbances propagating outward from a selected portion of the soil medium surrounding the structure of interest. The resulting set of first-order ordinary differential equations is then combined with the second-order equations of motion for the finite-element model so as to facilitate solution by a *staggered solution procedure*. This procedure is shown to be computationally stable as long as the time increment is smaller than a limiting value based on the finite-element mass matrix and the DAA-boundary stiffness matrix. Computational results produced by the boundary are compared with exact results for linear canonical problems pertaining to infinite-cylindrical and spherical shells.

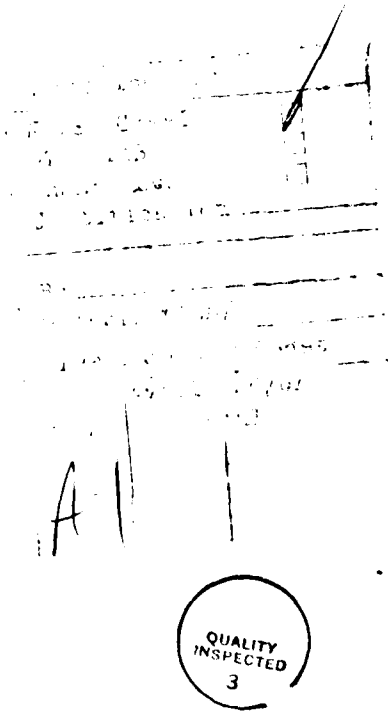

## PREFACE

This effort was carried out under Contract Number DNA 001-83-C-0239 with Dr. Kent L. Goering as Contract Technical Monitor. The authors appreciate Dr. Goering's support of their efforts, as well as the contributions of their colleages at Lockheed. In particular, Dr. K. C. Park helped to design the staggered solution procedure used to integrate the augmented doubly asymptotic equations of motion, Dr. C. A. Felippa provided consultation on the use of *NICE* integrated software, and Dr. C.-L. Yen provided exact solutions for the embedded spherical shell problem.

## TABLE OF CONTENTS

## TABLE OF CONTENTS (Concluded)

## LIST OF ILLUSTRATIONS

# SECTION 1

# INTRODUCTION

The primary objective of this effort has been the implementation of a *non-reflecting boundary* for use with existing finite-element codes to perform nonlinear ground-shock analyses of buried structures. This boundary is based on the *first-order doubly asymptotic approximation ($DAA_1$)* for elastodynamic scattering [*Geers and Yen (1981)*, *Underwood and Geers (1981)*]. In addition, a staggered solution procedure is utilized to partition the global equations in order to achieve both computational efficiency and software modularity [*Felippa and Park (1980)*].

This work extends that of *Underwood and Geers (1981)* for linear ground-shock problems, wherein the DAA surface is placed *on the surface* of the buried structure. Here, the DAA surface is moved some distance *out from the surface* of the structure, enclosing both the structure and a portion of the surrounding soil medium, which may be treated with nonlinear finite elements. Other extensions include formulation and implementation for general 2-D and 3-D problems, improved discretization of the DAA surface with higher-order interpolation functions, and utilization of a conditionally stable staggered-solution procedure.

## 1.1 Doubly Asymptotic vs. Singly Asymptotic Approximations

It is important to differentiate between doubly asymptotic approximations, which address quasi-static and wave-propagation effects simultaneously, and singly asymptotic approximations, which address these effects separately [see, e.g., various papers in *Kalinowski, ed. (1981)* and *Datta, ed., (1982)*, and *Cohen and Jennings (1983)*] For example, representation of the external medium by an elastic foundation, which may be quite satisfactory at low frequencies, does not account, at higher frequencies, for energy dissipation through outward propagation of scattered waves. On the other hand, representation of the external medium by a viscous boundary, which may be quite satisfactory for wave-propagation problems, does not provide elastic restoring forces in the static limit.

A response-averaging method originally proposed by *Smith (1974)* and extended by *Cundall, et al. (1978)* also fails in the static limit. For example, consider the response of a rigid structure surrounded by an infinite, linear-elastic medium to an internal, quasi-static point force. A computational model for this problem might consist of the rigid structure surrounded by a portion of the medium enclosed by a non-reflecting boundary. If this boundary is that of Smith, the total response of the structure is the *average* of two responses, one dependent on the stiffness of the bounded portion of medium enclosed by a rigid boundary, and the other associated with the structure and bounded portion of medium floating freely in space. Unfortunately, the latter response grows indefinitely in the static limit because the freely floating system is not in static equilibrium. In contrast, doubly asymptotic approximations approach exactness in the static limit.

## 1.2 Outline of Remainder of Report

Section 2 of this report derives the first-order doubly asymptotic equations of motion for a buried structure excited by a transient incident wave. Section 3 deals with formation of the medium stiffness matrix required for the low-frequency component of $DAA_1$. The staggered-solution procedure and associated stability analysis are discussed in Section 4, which establishes the time-increment limitation of the conditionally stable algorithm. Section 5 describes the implementation of the formulation as computer software, and presents numerical results for two canonical problems, *viz.*, excitation of an infinite-cylindrical and a spherical shell by a plane dilatational wave. Section 6 concludes the report with some observations and recommendations for future work.

## SECTION 2

## GOVERNING EQUATIONS

This section presents the governing equations for the finite-element (FE) model of the structure along with a portion of the surrounding soil medium, and for the boundary-element model (BE) of the non-reflecting DAA surface. These equations are then partitioned, and a staggered-solution procedure is introduced to solve for transient response. Throughout the development, the dependence of excitation and response quantities on time is implicit.

### 2.1 Finite-Element/Boundary-Element Model

Let $\mathbf{x}$ be the *computational vector* of displacement response in global coordinates for the FE model of the structure and portion of surrounding medium. The governing equations for the finite-element model are then [see, *e.g., Zienkiewicz (1977)*]

$$\mathbf{M}_s\ddot{\mathbf{x}} + \mathbf{D}_s\dot{\mathbf{x}} + \mathbf{K}_s\mathbf{x} = \mathbf{f}_e + \mathbf{f}_i \tag{2.1}$$

where $\mathbf{M}_s$, $\mathbf{D}_s$ and $\mathbf{K}_s$ are the mass, damping and stiffness matrices, respectively, for the FE model, $\mathbf{f}_e$ is the computational vector of external medium forces imposed by the DAA surface and $\mathbf{f}_i$ is the vector of internal nonlinear forces: as usual, a dot denotes differentiation in time. Compatibility of forces and displacements at the DAA surface may be expressed as [*Geers and Underwood (1981)*]

$$\begin{aligned} \mathbf{f}_e &= -\mathbf{G}\mathbf{g} \\ \mathbf{u} &= \mathbf{G}^T\mathbf{x} \end{aligned} \tag{2.2}$$

where $\mathbf{g}$ and $\mathbf{u}$ are the global force and displacement vectors, respectively, for the BE model of the DAA surface and $\mathbf{G}$ is the force-transformation matrix from BE to FE coordinates.

Now the force vector $\mathbf{g}$ and displacement vector $\mathbf{u}$ may be decomposed into incident-wave and scattered-wave components as

$$\begin{aligned} \mathbf{g} &= \mathbf{g}_I + \mathbf{g}_S \\ \mathbf{u} &= \mathbf{u}_I + \mathbf{u}_S \end{aligned} \tag{2.3}$$

where $\mathbf{g}_I$ is the *known* force vector associated with a free-field incident wave and $\mathbf{g}_S$ is the *unknown* force vector associated with the wave scattered by the structure. It is worth noting that this dual decomposition does not require constitutive linearity of the medium to be valid, for $\mathbf{g}_S$ and $\mathbf{u}_S$ may each be viewed as merely the difference between two vectors, one obtaining with the structure absent and the other obtaining with the structure present.

### 2.2 Doubly Asymptotic Approximation

A first-order DAA is used here to relate the scattered-force vector $\mathbf{g}_S$ and the scattered-displacement vector $\mathbf{u}_S$ [*Geers and Yen (1981)* and *Underwood and Geers (1981)*]. This

approximation approaches exactness in both the high- and low-frequency limits, and effects a smooth transition between. The development of $DAA_1$ for a linear, isotropic external medium proceeds as follows.

At *high frequencies*, the *geometrical vector* of scattered-wave surface tractions for the DAA surface corresponding to normal and tangential motions of that surface is given by

$$t'_S(p) = \rho_m C_m \dot{u}'_S(p) \tag{2.4}$$

where $p$ denotes a point on the surface, $\rho_m$ is the mass density of the medium, and $C_m$ is the diagonal sound-speed matrix corresponding to $\dot{u}'_S$, which is the geometrical vector of normal and tangential scattered-wave velocities. For the component of $\dot{u}'_S$ normal to the DAA surface, the corresponding matrix component is the dilatational velocity, while for each component of $\dot{u}'_S$ tangential to the DAA surface, the corresponding matrix component is the shear velocity.

Now the local-coordinate vectors of (2.4) may be transformed into global-coordinate vectors as

$$u'_S(p) = Q(p)\, u_S(p), \qquad t'_S(p) = Q(p)\, t_S(p) \tag{2.5}$$

to obtain, inasmuch as $Q^{-1} = Q^t$, where the superscripts $-1$ and $t$ denote inverse and transpose, respectively.

$$t_S(p) = Q^t(p)\, \rho_m C_m\, Q(p)\, \dot{u}_S(p) \tag{2.6}$$

Hence boundary-element discretization of $u_S$ as (see, *e.g.*, *Zienkiewicz (1977)*)

$$u_S(p) = \mathbf{N}(p)\mathbf{u}_S \tag{2.7}$$

where $\mathbf{N}(p)$ is a matrix of shape-functions and $\mathbf{u}_S$ is a vector of displacement degrees of freedom, and definition of the high-frequency scattered-wave force vector as

$$\mathbf{g}_S^h = \int \mathbf{N}^t(p)\, t_S(p)\, dS \tag{2.8}$$

yield, for high-frequency motions,

$$\mathbf{g}_S^h = \mathbf{D}_m \dot{\mathbf{u}}_S \tag{2.9}$$

in which

$$\mathbf{D}_m = \int \mathbf{N}^t\, Q^t\, \rho_m C_m\, Q\, \mathbf{N}\, dS \tag{2.10}$$

At *low frequencies*, the scattered-wave force computational vector is given by the quasi-static relation

$$\mathbf{g}_S^l = \mathbf{K}_m \mathbf{u}_S \tag{2.11}$$

where $\mathbf{K}_m$ is a full, nonsymmetric stiffness matrix for the boundary-element mesh, whose construction is described in the next section.

Finally, the first-order doubly asymptotic approximation $\mathrm{DAA}_1$ is formed by the superposition of $\mathbf{g}_S^l$ and $\mathbf{g}_S^h$ to obtain

$$\mathbf{g}_S = \mathbf{D}_m \dot{\mathbf{u}}_S + \mathbf{K}_m \mathbf{u}_S \tag{2.12}$$

Now the assumption embodied in $\mathrm{DAA}_1$ of a constitutively linear medium for the scattered wave is justified within the framework of classical plasticity theory if the material point for every exterior location, *i.e.*, every location in the medium outside the DAA surface, remains within its corresponding yield surface when and after the scattered wave arrives at the DAA surface. For incident waves with sufficiently rapid decay rates and for a DAA surface sufficiently removed from the surface of the structure, the scattered wave causes minor perturbations about an elastic state at each exterior location, thereby satisfying the preceding condition.

The assumption of material isotropy outside the DAA surface cannot be rigorously maintained if the material has suffered plastic excursions in response to the incident wave. However, it is likely that the resulting anisotropy is no more pronounced than that characterizing the ambient state, which is generally uncertain in practical cases. Hence, while an extension to material orthotropy may be theoretically possible, it may not be worth the trouble.

### 2.3 Response Equations

Introduction of the first of (2.2) and (2.3) into (2.1) and of the second of (2.2) and (2.3) into (2.12) yields the *doubly asymptotic equations of motion*

$$\begin{aligned} \mathbf{M}_s \ddot{\mathbf{x}} + \mathbf{D}_s \dot{\mathbf{x}} + \mathbf{K}_s \mathbf{x} &= -\mathbf{G}\{\mathbf{g}_I + \mathbf{g}_S\} + \mathbf{f}_t \\ \mathbf{g}_S &= \mathbf{D}_m\{\mathbf{G}^T \dot{\mathbf{x}} - \dot{\mathbf{u}}_I\} + \mathbf{K}_m\{\mathbf{G}^T \mathbf{x} - \mathbf{u}_I\} \end{aligned} \tag{2.13}$$

which may be numerically integrated in time to obtain the solution vectors $\mathbf{x}$ and $\mathbf{g}_S$. Because $\mathbf{M}_s$, $\mathbf{D}_s$ and $\mathbf{K}_s$ are typically large and banded, while $\mathbf{K}_m$ is relatively small and full, it is not computationally practical to introduce the second of these equations into the first to eliminate $\mathbf{g}_S$.

However, because $\mathbf{D}_m$ is banded and multiplies the highest-derivative terms in the second of (2.13), it is advantageous to apply the technique of *augmentation* Park, *et al.* (1977), which here merely involves introducing the second of (2.13) into the first, moving the term containing $\mathbf{D}_m$ to the left side of the resulting set of equations, and keeping $\mathbf{G}\mathbf{K}_m\mathbf{G}^T\mathbf{x}$ on the right. This yields the *augmented doubly asymptotic equations of motion*

$$\mathbf{M}_s\ddot{\mathbf{x}} - [\mathbf{D}_s + \mathbf{G}\mathbf{D}_m\mathbf{G}^t]\dot{\mathbf{x}} + \mathbf{K}_s\mathbf{x} = -\mathbf{G}\mathbf{g}_I + \mathbf{G}\mathbf{D}_m\dot{\mathbf{u}}_I + \mathbf{G}\mathbf{K}_m\mathbf{u}_I + \mathbf{f}_t - \mathbf{G}\mathbf{K}_m\mathbf{G}^t\mathbf{x} \quad (2.14)$$

which are highly amenable to staggered solution, as discussed in Section 4.

# SECTION 3

# MEDIUM STIFFNESS MATRIX

This section describes the construction of the boundary-element stiffness matrix that relates the scattered-wave force and displacement vectors at low frequencies. The development is based on Somigliana's identities, which derive from Betti's reciprocal work theorems and Kelvin's problem of a point load in an infinite elastic medium [see, e.g., *Kupradze (1965), Rizzo (1967), Cruse (1969), Lachat and Watson (1976)*]

## 3.1 Elastostatic Boundary-Integral Equations

The surface behavior of an elastic medium, whether occupying an exterior or interior region, may be expressed as [*Rizzo (1967), Cruse (1969)*]

$$c(p)u(p) + \int_\Gamma T(p,q)u(q)\,d\Gamma_q = \int_\Gamma U(p,q)t(q)\,d\Gamma_q \tag{3.1}$$

where $p$ is a point on the boundary and $q$ is the integration variable, and where $u(p)$ and $t(p)$ are $d \times 1$ vectors ($d = 2$ or 3) of medium displacements and tractions in Cartesian coordinates on the boundary at $p$. The elements $T_{ij}(p,q)$ and $U_{ij}(p,q)$ of the $d \times d$ matrices $T(p,q)$ and $U(p,q)$ are fundamental solutions for the tractions and displacements at a location $q$ in the direction $i$ due to a point load at location $p$ in direction $j$. With $\delta_{ij}$ as the Kronecker symbol, each element of the matrix $c$ is defined as

$$c_{ij}(p) = \tfrac{1}{2}\delta_{ij} \tag{3.2}$$

if there exists a continuous tangent at $p$, or, with $\Gamma_\epsilon$ as the surface of a sphere of radius $\epsilon$ centered at $p$,

$$c_{ij}(p) = \lim_{\epsilon \to 0} \int_\Gamma T_{ij}(p,q)\,d\Gamma_q \tag{3.3}$$

if the tangent is not continuous. A simple method for the evaluation of $c_{ij}$ is given in Appendix A.

Now an element of the *two-dimensional* displacement-kernel matrix $U(p,q)$ for plane-strain problems is given by

$$U_{ij}(p,q) = \frac{-1}{8\pi(1-\nu)G}\left[(3-4\nu)ln(r)\delta_{ij} - r_{,i}\,r_{,j}\right] \tag{3.4}$$

where $G$ and $\nu$ are the shear modulus and Poisson's ratio,respectively, and $r = r(p,q)$ is the distance between the load point $p$ and the field point $q$; the derivatives are taken with reference to the coordinates of $q$. With $p_i$ and $q_i$ as the coordinates of $p$ and $q$, respectively,

$$
\begin{aligned}
r_i &= q_i - p_i \\
r &= (r_i r_i)^{\frac{1}{2}} \\
r_{,i} &= \frac{q_i - p_i}{r}
\end{aligned}
\tag{3.5}
$$

In contrast, an element of the *three-dimensional* displacement-kernel matrix $U(p,q)$ is given by

$$
U_{ij}(p,q) = \frac{1}{16\pi(1-\nu)G\,r}\left[(3-4\nu)\delta_{ij} + r_{,i}\,r_{,j}\right] \tag{3.6}
$$

Finally, an element of the traction-kernel matrix $T(p,q)$ for *both two- and three-dimensional* problems is given by

$$
T_{ij}(p,q) = \frac{-1}{4\alpha\pi(1-\nu)r^{\alpha}}\left\{\left[(1-2\nu)\delta_{ij} + \beta r_{,i}\,r_{,j}\right]r_{,i}\,n_i - (1-2\nu)(r_{,i}\,n_j - r_{,j}\,n_i)\right\} \tag{3.7}
$$

where $n_i$ and $n_j$ are direction-cosines for the surface normal at $q$. The two- and three-dimensional forms are explicitly obtained by letting $\alpha = 1, 2$ and $\beta = 2, 3$, respectively.

### 3.2 Discretization

Numerical solution of the integral equation (3.1) requires discretization of the DAA surface, over each boundary element of which the displacement and traction vectors are approximated. The curved isoparametric elements of finite-element theory offer both the generality and the accuracy needed for this purpose. With this approach, the global Cartesian coordinates of any point in an element are taken as related to the nodal coordinates by *c.f.* (2.7)

$$
x(p) = \mathbf{N}(p)\ \mathbf{x} \tag{3.8}
$$

*i.e.*, the same shape functions are used to approximate element geometry, displacements and tractions. This allows interpolated displacements and tractions along the DAA curve in two-dimensional space to be integrated over a normalized length in $\xi$-coordinate space, and similar quantities over the DAA surface in three-dimensional space to be integrated over a standard $2 \times 2$ normalized square in $\xi_1, \xi_2$-coordinate space.

On an element-by-element basis, (3.8) becomes

$$
x^e(\xi^e) = \sum_k N_k(\xi^e)\ \mathbf{x}_k^e \tag{3.9}
$$

where $x^e(\xi^e)$ is the $d \cdot 1$ vector of Cartesian coordinates of a point in element $e$, the $N_k(\xi^e)$ are the element shape functions, and $\mathbf{x}_k^e$ is the $d \cdot 1$ vector of Cartesian coordinates of the $k$th element node; also, $\xi^e = \xi^e$ in 2-D, but $\xi^e = \xi_1^e, \xi_2^e$ in 3-D. The elements used in this

study are the three-noded, quadratic, curved element for 2-D analysis and the eight-noded, quadratic, serendipity element for 3-D analysis. The shape functions for the three-noded quadratic element are

$$\begin{aligned} N_1 &= \tfrac{1}{2}\xi(\xi - 1) \\ N_2 &= 1 - \xi^2 \\ N_3 &= \tfrac{1}{2}\xi(\xi + 1) \end{aligned} \tag{3.10}$$

where $\xi \in$ [-1,1]; the nodes are located at $\xi$ = -1,0,1. The shape functions for the eight-noded quadratic element are

$$\begin{aligned} N_1 &= -\tfrac{1}{4}(1 - \xi_1)(1 - \xi_2)(1 + \xi_1 + \xi_2) \\ N_2 &= \tfrac{1}{2}(1 - \xi_1^2)(1 - \xi_2) \\ N_3 &= \tfrac{1}{4}(1 + \xi_1)(1 - \xi_2)(\xi_1 - \xi_2 - 1) \\ N_4 &= \tfrac{1}{2}(1 + \xi_1)(1 - \xi_2^2) \\ N_5 &= \tfrac{1}{4}(1 + \xi_1)(1 + \xi_2)(\xi_1 + \xi_2 - 1) \\ N_6 &= \tfrac{1}{2}(1 - \xi_1^2)(1 + \xi_2) \\ N_7 &= \tfrac{1}{4}(1 - \xi_1)(1 + \xi_2)(-\xi_1 - \xi_2 - 1) \\ N_8 &= \tfrac{1}{2}(1 - \xi_1)(1 - \xi_2^2) \end{aligned} \tag{3.11}$$

where $\xi_1 \in$ [-1,1] and $\xi_2 \in$ [-1,1], and all nodes lie at the intersections of the $\xi_1$ = -1.0.1 and the $\xi_2$ = -1,0,1 lines, except at 0,0, where there is no node.

### 3.3 Matrix Assembly

With DAA-surface coordinates, displacements and tractions approximated as

$$x(p) = \mathbf{N}(p)\mathbf{x} \qquad u(p) = \mathbf{N}(p)\mathbf{u} \qquad t(p) = \mathbf{N}(p)\mathbf{t} \tag{3.12}$$

(3.1) may be expressed at a node $P$ as

$$\begin{aligned} c(P)u(P) - \sum_{e=1}^{E} \int_{\Gamma_e} T(P, q\,\xi^e)\ \sum_k N_k(\xi^e)\,\mathbf{u}_k^e\ J(\xi^e)\,d\xi^e \\ = \sum_{e=1}^{E} \int_{\Gamma_e} U(P, q\,\xi^e)\ \sum_k N_k(\xi^e)\,\mathbf{t}_k^e\ J(\xi^e)\,d\xi^e \end{aligned} \tag{3.13}$$

where $E$ is the total number of elements on the DAA surface and $J(\xi^e)$ is the Jacobian for $\mathbf{x}^e - \xi^e$ transformation: also, $d\xi^e = d\xi^e$ in 2-D, but $d\xi^e = d\xi_1^e d\xi_2^e$ in 3-D. Finally, coalescence of element contributions at common nodes is implicit in (3.13). The numerical techniques used to evaluate the integrals in this equation are discussed in Appendix A.

Evaluation of (3.13) at every node on the DAA surface yields a set of simultaneous algebraic equations that can be expressed in the form

$$\mathbf{A}\,\mathbf{u} = \mathbf{B}\,\mathbf{t} \tag{3.14}$$

so that

$$\mathbf{t} = \mathbf{B}^{-1}\mathbf{A}\mathbf{u} \tag{3.15}$$

Now the nodal force vector $\mathbf{g}$ corresponding to a traction distribution $t$ on the DAA surface is given by

$$\mathbf{g} = \int_{\Gamma} \mathbf{N}^t(p)\, t(p)\, d\Gamma \tag{3.16}$$

Introduction of the third of (3.12) and of (3.15) into this relation then yields

$$\mathbf{g} = \mathbf{K}_m\mathbf{u} \tag{3.17}$$

where the generally non-symmetric medium stiffness matrix $\mathbf{K}_m$ is given by

$$\mathbf{K}_m = \left[\int_{\Gamma} \mathbf{N}^t\mathbf{N}\, d\Gamma\right] \mathbf{B}^{-1}\mathbf{A} \tag{3.18}$$

A symmetric form may be obtained as

$$\hat{\mathbf{K}}_m = \tfrac{1}{2}(\mathbf{K}_m - \mathbf{K}_m^t) \tag{3.19}$$

which is identical to that derived from energy considerations [*Zienkiewicz, Kelly and Bettess (1977)*]. As indicated in Appendix B, however, the use of $\hat{\mathbf{K}}_m$ generally yields numerical results inferior to those produced by $\mathbf{K}_m$.

# SECTION 4

# STAGGERED SOLUTION PROCEDURE

In the interest of computational efficiency, the augmented doubly asymptotic equations of motion given by (2.14) are solved with a staggered solution procedure. The procedure is conditionally stable, requiring that the time increment be smaller than the shortest *medium-boundary period* divided by $\pi$. This shortest period may be obtained by determining the highest natural frequency for the eigenproblem

$$\omega^2 \mathbf{M}_s \mathbf{x} = \mathbf{G}\mathbf{K}_m\mathbf{G}^t\mathbf{x} \tag{4.1}$$

In cases where the surrounding soil does not appreciably stiffen the embedded structure beyond its inherent level, the highest *medium-boundary frequency* is substantially lower than the highest natural frequency characterizing the structure itself, thereby allowing the analyst to carry out stable calculations with a relatively large time increment. The remainder of this section describes the staggered-solution procedure and the stability analysis that leads to (4.1).

## 4.1 Solution Algorithm

To construct the staggered solution procedure for (2.14), those equations are expressed at mid-step as

$$\mathbf{M}_s \ddot{\mathbf{x}}_{n+1/2} + \mathbf{D}_T \dot{\mathbf{x}}_{n+1/2} + \mathbf{K}_s \mathbf{x}_{n+1/2} = \mathbf{f}_{n+1/2} - \mathbf{K}_M \mathbf{x}_{n+1/2} \tag{4.2}$$

where the time step $n = t/\Delta t$, in which $t$ and $\Delta t$ are time and *fixed* time increment, respectively, and where the *total damping matrix* $\mathbf{D}_T$, the *medium-boundary stiffness matrix* $\mathbf{K}_M$, and the *total force vector* $\mathbf{f}$ are given by

$$\begin{aligned} \mathbf{D}_T &= \mathbf{D}_s + \mathbf{G}\mathbf{D}_m\mathbf{G}^t \\ \mathbf{K}_M &= \mathbf{G}\mathbf{K}_m\mathbf{G}^t \\ \mathbf{f} &= -\mathbf{G}\mathbf{g}_I + \mathbf{G}\mathbf{D}_m\dot{\mathbf{u}}_I + \mathbf{G}\mathbf{K}_m\mathbf{u}_I + \mathbf{f}_i \end{aligned} \tag{4.3}$$

The integration algorithm utilized is the *trapezoidal rule* (see, *e.g.*, *Henrici (1962)*), for which

$$\begin{aligned} \dot{\mathbf{x}}_{n+1/2} &= (\mathbf{x}_{n+1/2} - \mathbf{x}_n)/\delta \\ \ddot{\mathbf{x}}_{n+1/2} &= (\dot{\mathbf{x}}_{n+1/2} - \dot{\mathbf{x}}_n)/\delta \\ \mathbf{x}_{n+1} &= 2\mathbf{x}_{n+1/2} - \mathbf{x}_n \\ \dot{\mathbf{x}}_{n+1} &= 2\dot{\mathbf{x}}_{n+1/2} - \dot{\mathbf{x}}_n \end{aligned} \tag{4.4}$$

where $\delta = \Delta t/2$. Introduction of the first and then the last of these into the third yields the standard form

$$\mathbf{x}_{n+1} = \mathbf{x}_n + \frac{\Delta t}{2}(\dot{\mathbf{x}}_{n+1} + \dot{\mathbf{x}}_n) \tag{4.5}$$

Now the first two of (4.4) are introduced into the left side of (4.2) and $\mathbf{x}_{n+1/2}$ on the right side of (4.2) is *predicted* as $\mathbf{x}^p_{n+1/2}$ to obtain the set of algebraic equations

$$\mathbf{E}_l \mathbf{x}_{n+1/2} = \mathbf{e}_{n+1/2} - \mathbf{E}_r \mathbf{x}^p_{n+1/2} \tag{4.6}$$

where

$$\begin{aligned} \mathbf{E}_l &= \mathbf{M}_s + \delta \mathbf{D}_T + \delta^2 \mathbf{K}_s \\ \mathbf{E}_r &= \delta^2 \mathbf{K}_M \\ \mathbf{e}_{n+1/2} &= \delta^2 \mathbf{f}_{n+1/2} + \mathbf{M}_s(\mathbf{x}_n + \delta \dot{\mathbf{x}}_n) + \delta \mathbf{D}_T \mathbf{x}_n \end{aligned} \tag{4.7}$$

Finally, the prediction $\mathbf{x}^p_{n+1/2}$ is based on the *one-term extrapolation*

$$\mathbf{x}^p_{n+1/2} = \mathbf{x}_n \tag{4.8}$$

The preceding staggered solution procedure leads to the following computational sequence to determine system response at time step $n - 1$:

*(a)* $\mathbf{f}_{n+1/2} = (\mathbf{f}_n + \mathbf{f}_{n-1})/2$

*(b)* $\mathbf{e}_{n+1/2} = \delta^2 \mathbf{f}_{n+1/2} - \mathbf{M}_s(\mathbf{x}_n + \delta \dot{\mathbf{x}}_n) - \delta \mathbf{D}_T \mathbf{x}_n$

*(c)* $\mathbf{x}^p_{n+1/2} = \mathbf{x}_n$

*(d)* $\mathbf{x}_{n+1/2} = \mathbf{E}_l^{-1}(\mathbf{e}_{n+1/2} - \mathbf{E}_r \mathbf{x}^p_{n+1/2})$

*(e)* $\mathbf{x}_{n-1} = 2\mathbf{x}_{n+1/2} - \mathbf{x}_n$

*(f)* $\dot{\mathbf{x}}^c_{n-1/2} = (\mathbf{x}_{n-1/2} - \mathbf{x}_n)/\delta$

*(g)* $\ddot{\mathbf{x}}_{n-1/2} = \mathbf{M}_s^{-1}(\mathbf{f}_{n-1/2} - \mathbf{D}_T \dot{\mathbf{x}}^c_{n-1/2} - \mathbf{K}_T \mathbf{x}_{n-1/2})$

*(h)* $\dot{\mathbf{x}}_{n+1/2} = \dot{\mathbf{x}}_n + \delta \ddot{\mathbf{x}}_{n-1/2}$

*(i)* $\dot{\mathbf{x}}_{n-1} = 2\dot{\mathbf{x}}_{n-1/2} - \dot{\mathbf{x}}_n$

where the *total stiffness matrix* $\mathbf{K}_T = \mathbf{K}_s - \mathbf{K}_M$. To improve accuracy, an iterative loop has been introduced at *(d)*, wherein $\mathbf{x}^p_{n-1/2}$ on the right is corrected to the previously calculated value of $\mathbf{x}_{n+1/2}$; two iterations generally produce satisfactory convergence. The calculation starts at $n = 0$ with $\mathbf{x}_0 = \dot{\mathbf{x}}_0 = 0$.

## 4.2 Stability Analysis

*Park (1980)* has performed a stability analysis of a generalized form of the staggered solution procedure just described. The result is that the procedure is computationally stable if no root of the characteristic equation

$$det\left[ z^2(\mathbf{M}_s - \delta^2\mathbf{K}_M) - z\delta\,\mathbf{D}_T - \delta^2\mathbf{K}_T \right] = 0 \tag{4.9}$$

has a positive real part. Verification of this condition is relatively straightforward when all of the matrices in (4.9) are symmetric; it is generally quite difficult when one or more is not. Unfortunately, as discussed in Section 3, the medium stiffness matrix $\mathbf{K}_m$ is nonsymmetric, which pollutes $\mathbf{K}_M$ and $\mathbf{K}_T$. Fortunately, however, $\mathbf{K}_m$ constitutes a small perturbation of $\hat{\mathbf{K}}_m$, which *is* symmetric; hence it is appropriate to consider the characteristic equation

$$det\left[ z^2(\mathbf{M}_s - \delta^2\hat{\mathbf{K}}_M) - z\delta\,\mathbf{D}_T - \delta^2\hat{\mathbf{K}}_T \right] = 0 \tag{4.10}$$

where $\hat{\mathbf{K}}_M = \mathbf{G}\hat{\mathbf{K}}_m\mathbf{G}^t$ and $\hat{\mathbf{K}}_T = \mathbf{K}_s - \hat{\mathbf{K}}_M$.

As discussed on page 255 of *Bellman (1970)*, no root of (4.10) has a positive real part if $(\mathbf{M}_s - \delta^2\hat{\mathbf{K}}_M)$, $\mathbf{D}_T$ and $\hat{\mathbf{K}}_T$ are all non-negative definite and either $(\mathbf{M}_s - \delta^2\hat{\mathbf{K}}_M)$ or $\hat{\mathbf{K}}_T$ is positive definite. On physical grounds, $\mathbf{D}_T$ and $\hat{\mathbf{K}}_T$ are both non-negative definite, but generally not positive definite. However, inasmuch as $\mathbf{M}_s$ *is* positive definite, $(\mathbf{M}_s - \delta^2\hat{\mathbf{K}}_M)$ is positive definite if $\delta$ is sufficiently small. The degree of smallness defines the *stability requirement*, as discussed next.

Consider the following *first eigenproblem*:

$$\hat{\mathbf{Q}}\mathbf{x} = \lambda\,\mathbf{x} \tag{4.11}$$

where $\hat{\mathbf{Q}} = \mathbf{M}_s^{-1}\hat{\mathbf{K}}_M$. This problem yields non-negative real eigenvalues and real eigenvectors. These eigenvectors may be assembled into a modal transformation matrix $\boldsymbol{\Psi}$ that diagonalizes $\hat{\mathbf{Q}}$ as $\boldsymbol{\Psi}^t\hat{\mathbf{Q}}\boldsymbol{\Psi} = \hat{\mathbf{Q}}^d$ and normalizes as $\boldsymbol{\Psi}^t\boldsymbol{\Psi} = \mathbf{I}$, the identity matrix. Hence the introduction into (4.11) of a transformation from physical to generalized coordinates as $\mathbf{x} = \boldsymbol{\Psi}\,\mathbf{y}$ and subsequent premultiplication through by $\boldsymbol{\Psi}^t$ yield the diagonal eigenvalue matrix

$$\boldsymbol{\Lambda}_Q = \hat{\mathbf{Q}}^d \tag{4.12}$$

Consider next the following *second eigenproblem*:

$$\hat{\mathbf{K}}_M\mathbf{x} = \lambda\mathbf{M}\,\mathbf{x} \tag{4.13}$$

whose eigenvalues and eigenvectors are the same as those of the first eigenproblem. Hence the transformation from physical to generalized coordinates and premultiplication through by $\boldsymbol{\Psi}^t$ yields

$$\boldsymbol{\Lambda}_{K/M} = (\mathbf{M}_s^d)^{-1}\hat{\mathbf{K}}_M^d \tag{4.14}$$

where $\mathbf{M}_s^d = \boldsymbol{\Psi}^t\mathbf{M}_s\boldsymbol{\Psi}$ and $\hat{\mathbf{K}}_M^d = \boldsymbol{\Psi}^t\hat{\mathbf{K}}_M\boldsymbol{\Psi}$; $\boldsymbol{\Lambda}_{K/M}$ is, of course, identical to $\boldsymbol{\Lambda}_Q$.

Finally, consider the following *third eigenproblem*:

$$(\mathbf{M}_s - \delta^2 \hat{\mathbf{K}}_M)\,\mathbf{x} = \lambda\,\mathbf{x} \tag{4.15}$$

Transformation and premultication through as before yields

$$\begin{aligned} \mathbf{\Lambda}_{M-K} &= \mathbf{M}_s^d - \delta^2 \hat{\mathbf{K}}_M^d \\ &= \mathbf{M}_s^d [\mathbf{I} - \delta^2 (\mathbf{M}_s^d)^{-1} \hat{\mathbf{K}}_M^d] \\ &= \mathbf{M}_s^d [\mathbf{I} - \delta^2 \mathbf{\Lambda}_{K/M}] \\ &= \mathbf{M}_s^d [\mathbf{I} - \delta^2 \mathbf{\Lambda}_Q] \end{aligned} \tag{4.16}$$

Hence the eigenvalues of $(\mathbf{M}_s - \delta^2 \hat{\mathbf{K}}_M)$ are all positive, and thus $(\mathbf{M}_s - \delta^2 \hat{\mathbf{K}}_M)$ is positive definite, if $\delta^2$ times the largest eigenvalue $\lambda_Q^{max}$ is less than unity. With $\lambda_Q^{max} = (\omega_Q^{max})^2$, this yields the *stability requirement*

$$\Delta t < \frac{2}{\omega_Q^{max}} \tag{4.17}$$

which is stated in slightly different terms at the beginning of this section.

Establishment of the stability requirement (4.17) for a symmetric medium stiffness matrix facilitates the estimation of a similar requirement for a non-symmetric one. Clearly, no root of (4.9) has a positive real part if $\delta$ is vanishingly small, as $\mathbf{M}_s$ is symmetric and positive definite, and $\mathbf{D}_T$ is symmetric and non-negative definite. Also, on physical grounds, the eigenvalues of $(\mathbf{M}_s)^{-1}\mathbf{K}_M$ must be real and non-negative. Finally, the eigenvalues for the three eigenproblems above differ only slightly from their counterparts when $\hat{\mathbf{K}}_M$ is replaced by $\mathbf{K}_M$ because, as illustrated in Appendix B, $\mathbf{K}_m$ constitutes a small perturbation of $\hat{\mathbf{K}}_m$. Hence, as $\delta$ is increased from zero, all the roots of (4.9) contain negative real parts until the stability requirement (4.17) is approached, where $\omega_Q^{max}$ now pertains to the use of $\mathbf{K}_m$.

# SECTION 5

# IMPLEMENTATION AND COMPUTATION

This section describes the techniques used to implement in software the approach delineated above, and presents numerical results generated by that software. Modern software-engineering techniques are used [*Felippa (1981)*], in order to facilitate extension to large-scale production analysis. The numerical results pertain to canonical problems involving plane, dilatational step-waves that envelop infinite-cylindrical and spherical shells (Figure 1). These problems possess known analytical solutions.

## 5.1 Software Implementation

The approach described in Sections 2, 3 and 4 is embodied in an assembly of of four software entities:

1. *Structural Matrix Generator:* The structural mass and stiffness matrices, $\mathbf{M}_s$ and $\mathbf{K}_s$ in (2.14), are generated by the finite-element code DIAL [*Ferguson and Cyr (1984)*]: $\mathbf{D}_s$ is neglected. The structural matrices and related data are read into a *NICE* global database [*Felippa (1982)*].
2. *Medium Matrix Generator:* The medium damping and stiffness matrices, $\mathbf{D}_m$ and $\mathbf{K}_m$ in (2.14), are generated by software developed as part of this study in the manner described above; the force-transformation matrix $\mathbf{G}$ is constructed as a correspondence table. These data are read into the *NICE* global database.
3. *Incident Field Generator:* The incident-wave displacement, velocity and force vectors, $\mathbf{u}_I$, $\dot{\mathbf{u}}_I$ and $\mathbf{g}_I$ in (2.14), are also generated by software developed as part of this study in the manner described below; as these are time-dependent vectors, they are calculated dynamically as the calculation proceeds. $\mathbf{f}_t$ is taken as zero.
4. *Staggered Solution Procedure:* The solution algorithm described in Subsection 4.1 is implemented as a *NICE* procedure using a command language interpreter [*Felippa (1983)*]. The matrix operations embedded in the algorithm are performed with a matrix utility processor for data in unblocked skyline format [*Felippa (1978)*].

The FE and BE models are constructed independently, although the element grids match at the boundary. Geometrical symmetry is exploited in both canonical problems.

## 5.2 Incident-Wave Vectors

A plane, dilational step-wave characterized by a velocity jump $V_o$ and propagating in the $x_1$-direction may be described in terms of a scalar potential as

$$\phi^I = -\frac{V_o}{2c_d}\,(c_d t - x_1 - a)^2\, H(c_d t - x_1 - a) \tag{5.1}$$

where $c_d$ is the dilatational speed in the elastic medium, $H$ is the Heaviside operator, and $-a$ is the point on the $x_1$-axis where the wave front is located at $t = 0$. The application of classical continuum formulas [*Achenbach (1973)*] yields for the components of the geometrical displacement and velocity vectors for the incident wave

$$u_i^I = \delta_{1i} \frac{V_o}{c_d} (c_d t - x_1 - a) H(c_d t - x_1 - a)$$
$$\dot{u}_i^I = \delta_{1i} V_o \, H(c_d t - x_1 - a) \tag{5.2}$$

Hence the elements of the computational vectors $\mathbf{u}_I$ and $\dot{\mathbf{u}}_I$ are given by (6.2) evaluated at the surface nodes.

Similarly, the components of the incident-wave stress tensor and geometrical surface-traction vector are given by [*Achenbach (1973)*]

$$\sigma_{ij}^I = -\delta_{ij} \frac{V_o}{c_d} (\lambda + 2\mu\delta_{1i}) \, H(c_d t - x_1 - a) \tag{5.3}$$
$$t_j^I = \sigma_{ij} n_i$$

where $\lambda$ and $\mu$ are the Lamé constants and the $n_i$ are the direction-cosines for the surface normal. Hence the computational vector $\mathbf{g}_I$ is given by (3.16).

### 5.3 Infinite Cylindrical Shell

The first canonical problem is that of an infinite cylindrical shell embedded in an elastic medium and excited by a transverse, plane, dilatational wave *Garnet and Crouzet-Pascal (1966)*. The parameter ratios for this problem are $E_s/E_m = 2.5$ (Young's modulus), $h/a = 0.01$ (shell thickness-to-radius), $\rho_s/\rho_m = 1.156$ (mass density), $\nu_m = 0.25$ and $\nu_s = 0.2$ (Poisson's); these pertain to a concrete shell in slow granite. The duration of the rectangular incident-wave pulse is $c_d t/a = 10$. A curved, three-noded shell element is used to model the shell, so that the FE/BE discretization employs *conforming elements*.

The first computational model for this problem places the DAA boundary directly on the shell in the manner of *Underwood and Geers (1981)*. The use of six curved quadratic elements over the half-model yields results that are virtually identical to those of *Underwood and Geers (1981)*, which were generated with twenty linear elements over the half-model. Figure 2 shows DAA and exact displacement-response histories; agreement is seen to be excellent.

The second computational model introduces eight-noded medium finite elements between the shell and the DAA boundary, which is located one shell radius out from the shell surface (Figure 3). The displacement-response histories thus produced are shown in Figure 4 as solid lines, along with their DAA counterparts from Figure 3, which are shown as dashed lines. It is seen that the use of medium finite elements degrades solution accuracy somewhat by introducing spurious oscillations caused by *ringing of the mesh*. A third computational model, which locates the DAA boundary three shell radii out from the shell surface, yields results that are even more oscillatory, although peak-response values are still satisfactory.

### 5.4 Spherical Shell

The second canonical problem is that of a spherical shell embedded in an elastic medium and excited by a plane dilatational wave *Grafton and Fox (1965), Geers and Yen (1981)*.

The parameter ratios for this problem are the same as those for the infinite cylindrical shell, and the duration of the rectangular incident-wave pulse is also $c_d t / a = 10$. An eight-noded Ahmad shell element is used to model the shell, so that this FE/BE discretization also employs *conforming elements.*

As previously, the first computational model for this problem places the DAA boundary directly on the shell; six eight-noded quadratic elements are used over the quarter-model of the shell (Figure 5). DAA-based displacement-response histories are compared with their exact counterparts in Figure 6, the latter having been generated in the manner of *Geers and Yen (1981)*. Here too, agreement is seen to be excellent.

The second computational model introduces twenty-noded medium finite elements between the shell and the DAA boundary, which is located one shell radius out from the shell surface (Figure 7). The displacement-response histories thus produced are shown in Figure 8 as solid lines, along with their DAA counterparts from Figure 6, which are shown as dashed lines. Here too, it is seen that the use of medium finite elements degrades solution accuracy by introducing spurious oscillations caused by *ringing of the mesh.*

# SECTION 6

# CONCLUSION

This report has documented the formulation and implementation of a non-reflecting boundary for use with existing finite-element codes to perform nonlinear ground-shock analyses of buried structures. The boundary is based on a first-order doubly asymptotic approximation ($DAA_1$) for disturbances propagating outward from a selected portion of the soil medium surrounding the structure of interest. The resulting set of first-order ordinary differential equations is then combined with the second-order equations of motion for the finite-element model so as to facilitate solution by a staggered solution procedure. This procedure is shown to be computationally stable as long as the time increment is smaller than a limiting value based on the finite-element mass matrix and the DAA-boundary stiffness matrix. Computational results produced by the boundary are compared with exact results for linear canonical problems pertaining to infinite-cylindrical and spherical shells.

## 6.1 Observations

It is appropriate here to offer some comments regarding the work described above:

1. As pointed out in the *Introduction*, doubly asymptotic approximations are clearly superior to singly asymptotic approximations, the former incorporating both radiative energy dissipation and elastic restoring forces, the latter accounting for only one or the other.
2. While the medium damping matrix may be interpreted in terms of local dashpots positioned on the DAA surface, the medium stiffness matrix is not so easily regarded: attempts to simplify the fully coupled nature of $\mathbf{K}_m$ merely degrade the validity of the low-frequency approximation.
3. Although it is tempting to use a symmetric medium stiffness matrix in DAA computations, the resulting loss of accuracy constitutes too high a price.
4. The computational stability requirement (4.17) is a generous one when the soil is substantially softer than the structural material; when this is not the case, however, more efficient computations might be realized with an unconditionally stable staggered solution procedure, which is yet to be developed.
5. The use of modern software-engineering techniques, as embodied in the *NICE* Integrated Software System, greatly facilitates the implementation of methods for the analysis of coupled systems.
6. The results for the linear canonical problems once again demonstrate the difficulty of propagating a discontinuous wave front through a finite-element grid and, in contrast, the good performance of a boundary-element grid located directly on the surface of the structure.

## 6.2 Future Work

Future R&D work in this area could profitably pursue the following paths:

1. The usefulness of the non-reflecting $DAA_1$ boundary in nonlinear problems should be more stringently assessed by applying it to nonlinear canonical problems; the challenge here is to find "exact" solutions for such problems against which to compare the approximate solutions.
2. A non-reflecting DAA boundary should be developed for a medium half-space, this for application in near-surface ground-shock analyses.
3. An unconditionally stable staggered solution procedure should be formulated for problems not amenable to the conditionally stable procedure.
4. A new approach should be sought for satisfactorily propagating discontinuous wave fronts through finite-element grids; failing this, the option, in *nonlinear* response problems, of placing the DAA grid directly on the surface of the structure [*Underwood and Geers (1980)*] should be revisited.

## SECTION 7

## LIST OF REFERENCES


Achenbach, J. D. (1973), *Wave Propagation in Elastic Solids*, North-Holland, Amsterdam.

Bellman, R. (1970), *Introduction to Matrix Analysis*, McGraw-Hill, New York.

Burton, A. J. (1976), "Numerical Solution of acoustic radiation problems" *National Physical Laboratory report* OC5/535.

Cohen, M. and Jennings, P. C. (1983), "Silent Boundary Methods for Transient Analysis", pp. 301-360 of Belytschko, T. and Hughes, T. J. R., ed., *Computational Methods for Transient Analysis*, North-Holland, New York, NY.

Cruse, T.A. (1969), "Numerical Solutions in Three Dimensional Elastostatics", *International Journal of Solids and Structures*, Vol. 5, pp.1259-1274.

Cundall, P. A., et al. (1978), "Solution of Infinite Dynamic Problems by Finite Modelling in the Time Domain", *Proceedings of the Second International Conference on Applied Numerical Modelling*, Madrid, Spain.

Datta, S. K., ed. (1982), *Earthquake Ground Motion and Its Effects on Structures*, AMD-Vol.53, American Society of Mechanical Engineers, New York, NY.

Felippa, C. A. and Park, K. C., (1980), "Staggered Transient Analysis Procedures for Coupled Mechanical Systems: Formulation", *Computer Methods in Applied Mechanics and Engineering*, Vol.24, pp. 61-111.

Felippa, C. A. (1981), "Architecture of a Distributed Analysis Network for Computational Mechanics", *Computers and Structures*, Vol.13, pp. 405-413.

Felippa, C. A. (1982), "The Global Database Manager EZ-GAL", *LMSC-D766995*, Lockheed Palo Alto Research Laboratory, Palo Alto, CA.

Felippa, C. A. (1983), "A Command Language for Applied Mechanics Processors", *LMSC-D878511*, Lockheed Palo Alto Research Laboratory, Palo Alto, CA.

Felippa, C. A. (1978), "SKYPUL Users Manual", *LMSC-D623146*, Lockheed Palo Alto Research Laboratory, Palo Alto, CA.

Ferguson, G. H. and Cyr, N. (1984), "DIAL User's Manual", *LMSC-D850112*, Rev.L2D8, Lockheed Missiles and Space Company, Sunnyvale, CA.

Garnet, H. and Crouzet-Pascal, J. (1966) "Transient Response of a Circular Cylinder of Arbitrary Thickness, in an Elastic Medium, to a Plane Dilatational Wave", *Journal of Applied Mechanics*, Vol. 33, pp. 521-531.

Geers, T. L. and Yen, C.-L. (1981), "Transient Excitation of Cylindrical and Spherical Shells Embedded in Elastic Media: Residual Potential and Doubly Asymptotic Solutions", *LMSC-D767735*, Lockheed Palo Alto Research Laboratory, Palo Alto, CA.

Grafton, P. E. and Fox, J. W. L. (1965) "Interaction of Ground Motion in an Elastic Soil with Buried Structures", *Paper No. 65-410*, AIAA.

Henrici, P. (1962), *Discrete Variable Methods in Ordinary Differential Equations*, John Wiley & Sons, New York.

Kalinowski, A. J., ed. (1981), *Computational Methods for Infinite Domain Media-Structure Interaction*, AMD-Vol.46, American Society of Mechanical Engineers, New York, NY.

Kupradze, V.D. (1965), *Potential Methods in the Theory of Elasticity*, D. Davey, London.

Lachat, J.C. and Watson, J.O. (1976), "Effective Numerical Treatment of Boundary Integral Equations: A Formulation for Three-Dimensional Elastostatics", *International Journal for Numerical Methods in Engineering*, Vol. 10, pp. 991-1005.

Park, K. C., et al. (1977), "Stabilization of Staggered Solution Procedures for Fluid-Structure Interaction Analysis", pp. 95-124 of Belytschko, T. and Geers, T. L., ed., *Computational Methods for Fluid-Structure Interaction Problems*, AMD-Vol.26, American Society of Mechanical Engineers, New York, NY.

Park, K. C. (1980), "Partitioned Transient Analysis Procedures for Coupled-Field Problems: Stability Analysis", *Journal of Applied Mechanics*, Vol. 47, pp. 370-376.

Rizzo, F.J. (1967), "An Integral Equation Approach to Boundary Value Problems of Classical Elastostatics", *Quarterly of Applied Mathematics*, Vol. 25, pp. 83-95.

Smith, W. D. (1974), "A Nonreflecting Plane Boundary for Wave Propagation Problems", *Journal of Computational Physics*, Vol. 15, pp. 492-503.

Takahasi, H. and Mori, M. (1973) "Quadrature formulas obtained by variable transformation" *Numerische Mathematik*, Vol 21, pp. 206-219.

Timoshenko, S. and Goodier, J. N. (1951), *Theory of Elasticity*, McGraw-Hill, New York.

Underwood, P. G. and Geers, T. L. (1980), "Doubly Asymptotic, Boundary-Element Analysis of Nonlinear Soil-Structure Interaction", pp. 413-422 of Shaw, R. P., *et al.*, ed., *Innovative Numerical Analysis for the Applied Engineering Sciences*, University Press of Virginia, Charlottesville.

Underwood, P. and Geers, T. L. (1981), "Doubly Asymptotic, Boundary-Element Analysis of Dynamic Soil-Structure Interaction", *International Journal of Solids and Structures*, pp. 687-697.

Zienkiewicz, O. C. (1977), *The Finite Element Method*, McGraw-Hill, London.

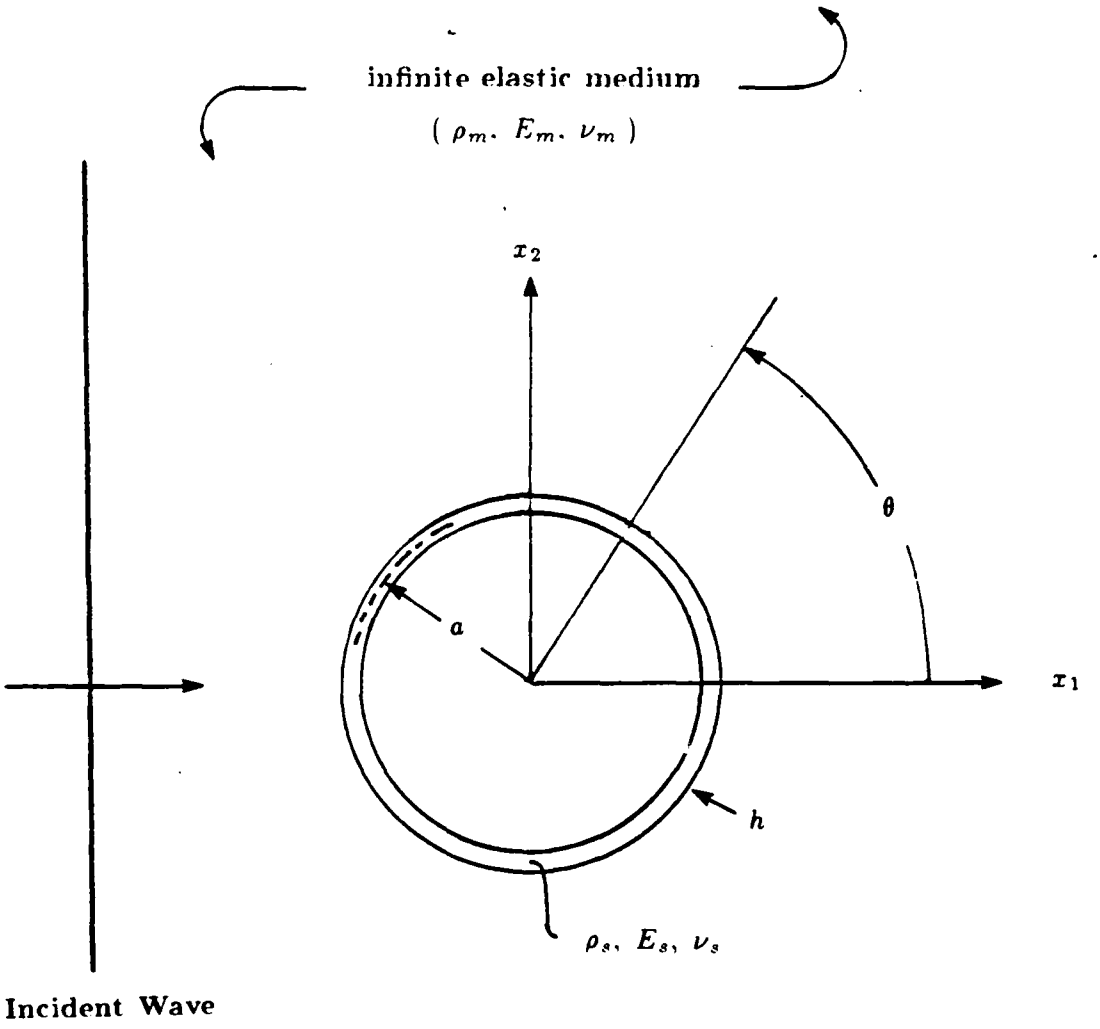


**Figure 1. Geometry and notation for canonical problems.**

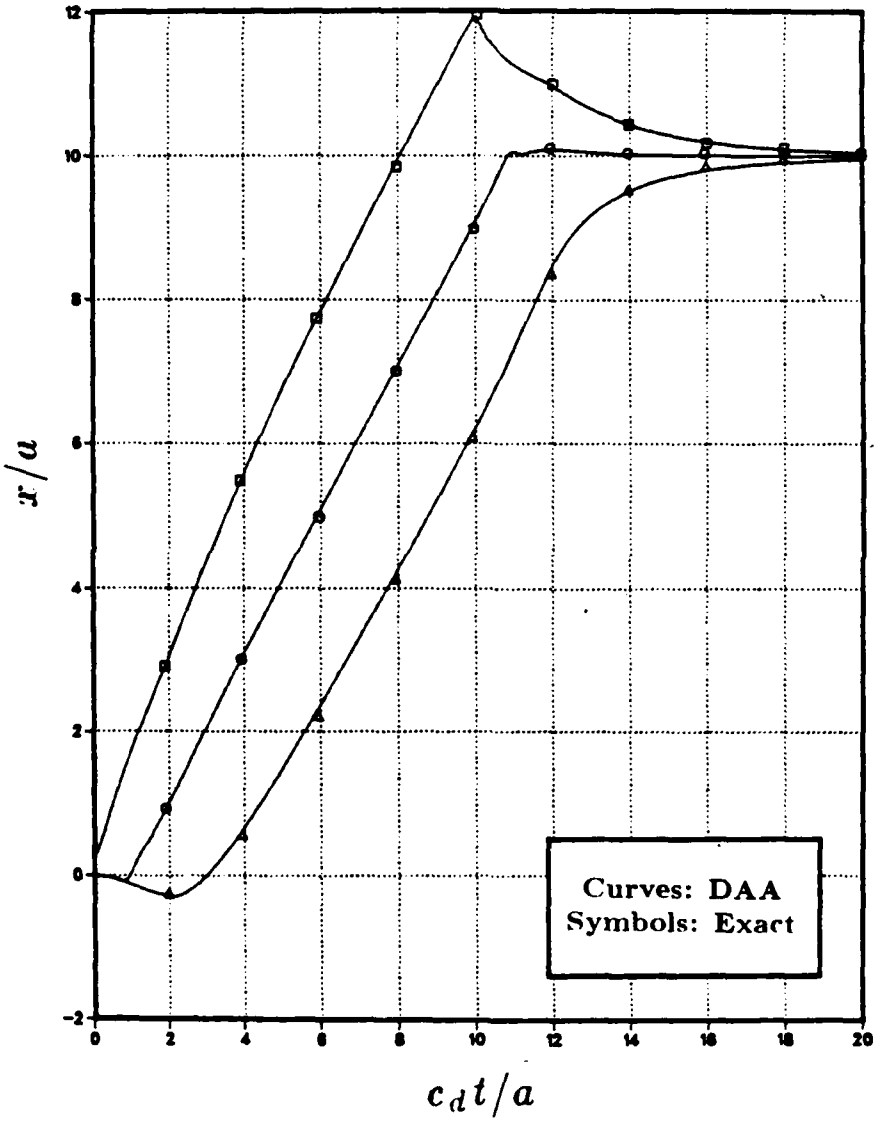


**Figure 2.** Displacement response histories for the infinite cylinderical shell (DAA boundary on shell surface).

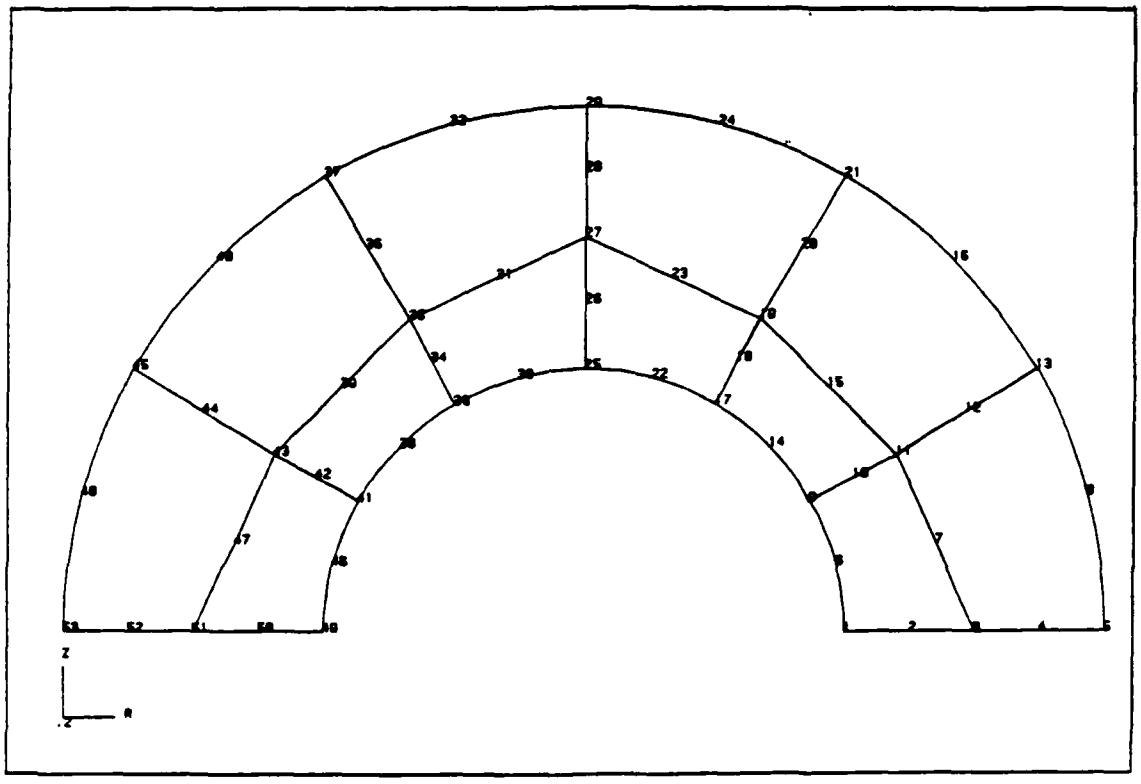

**Figure 3.** Half-model grid for the infinite cylinderical shell problem (finite elements extending to $r = 2a$).

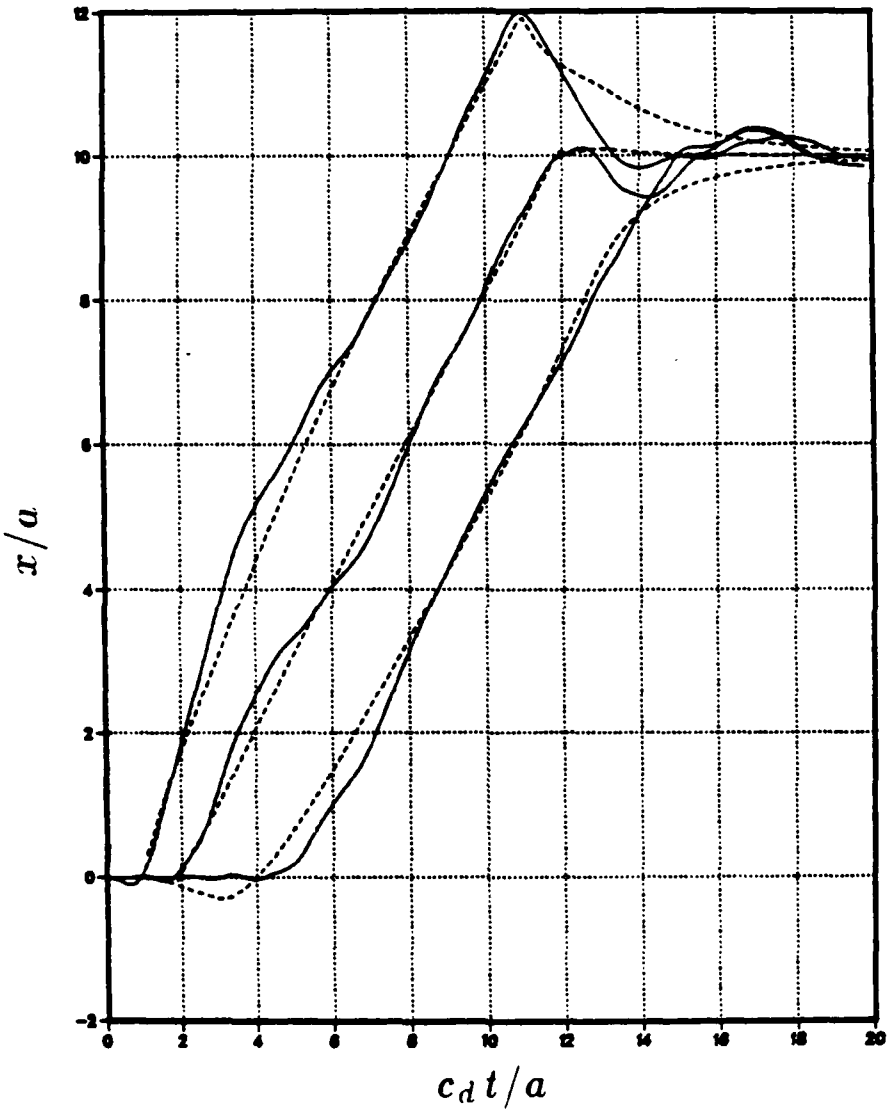


Figure 4. Displacement response histories for the infinite cylinderical shell (solid curves: finite elements around shell: dashed curves: DAA boundary on shell surface).

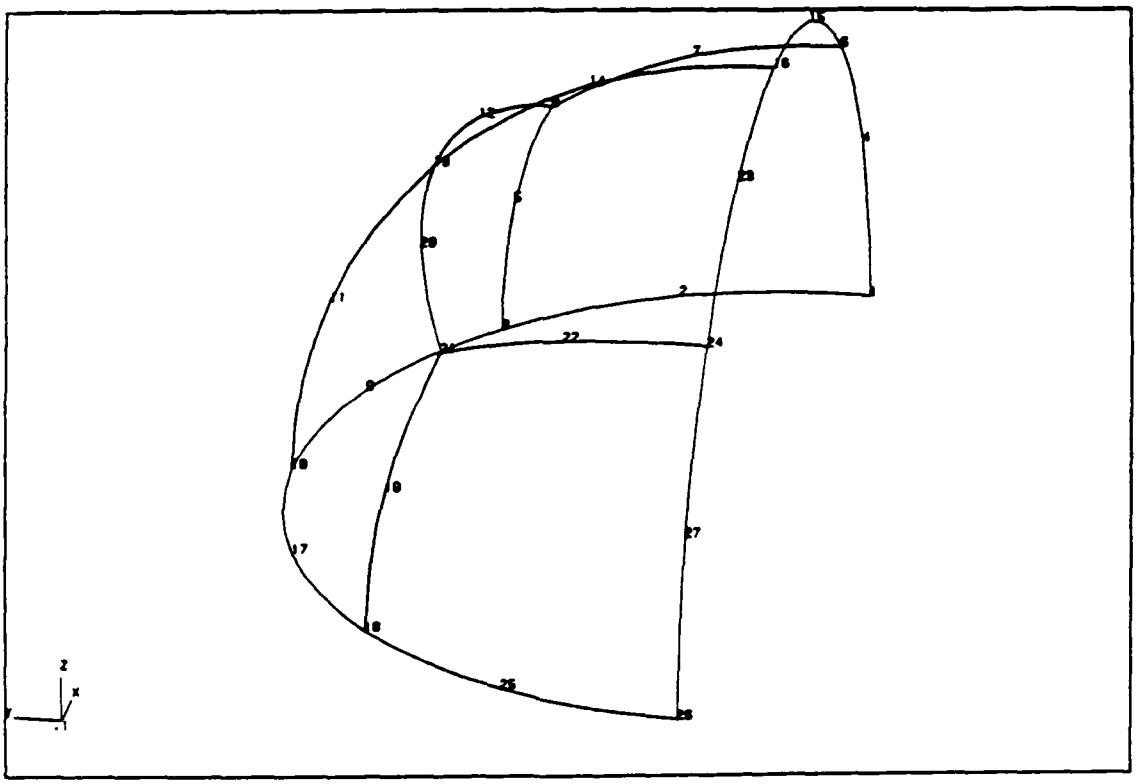

Figure 5. Quarter-model grid for the spherical shell problem (DAA boundary on shell surface).

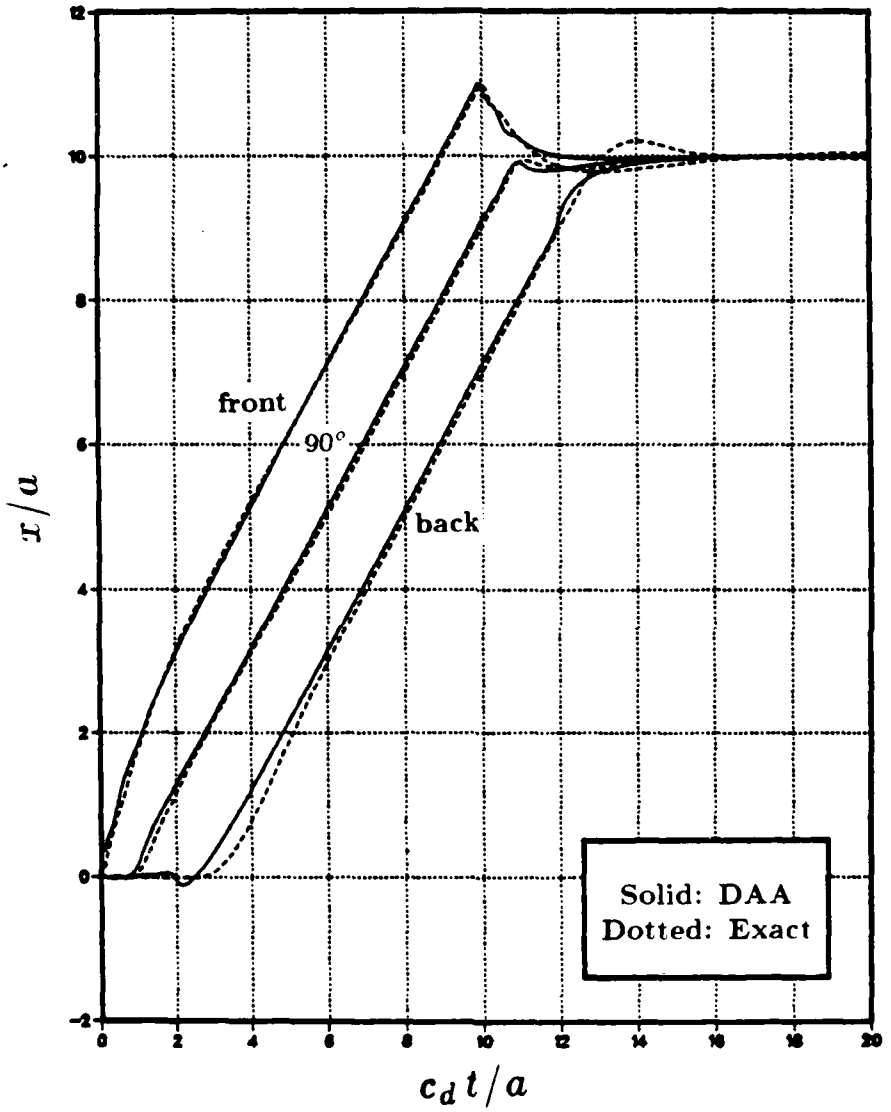


Figure 6. Displacemen response histories for spherical shell (DAA boundary on shell surface).

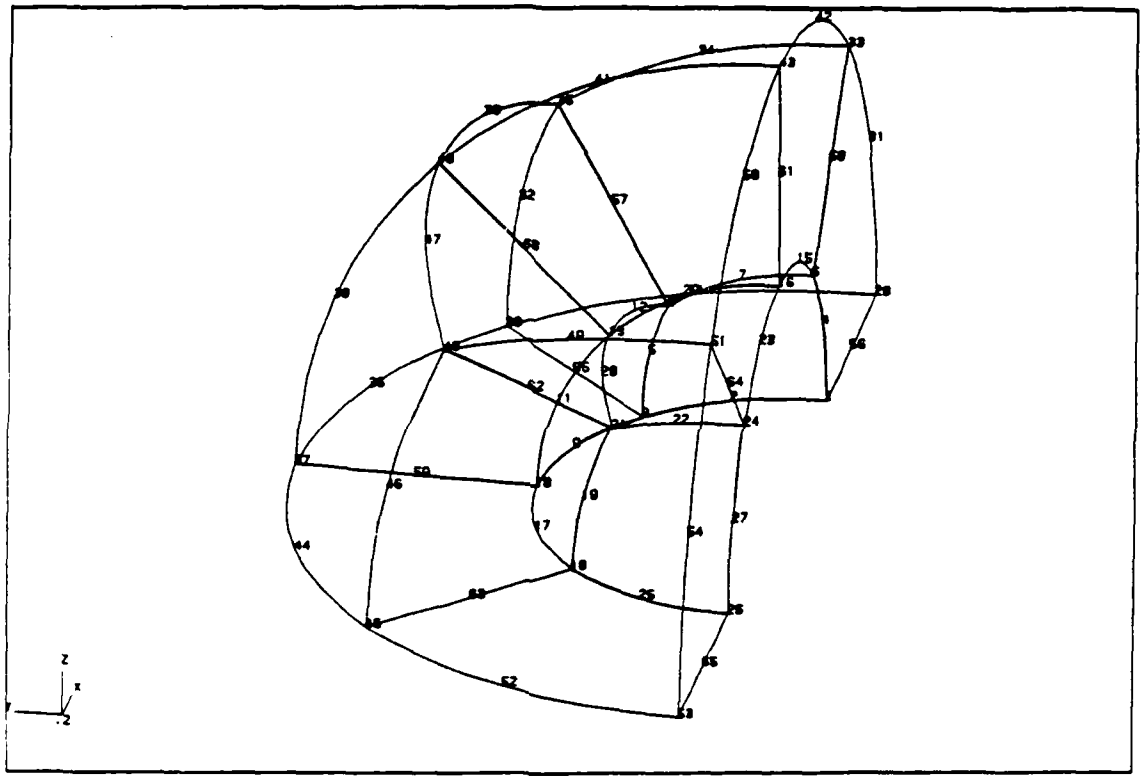

Figure 7. Quarter-model grid for spherical shell problem (Finite elements extending to $r = 2a$).

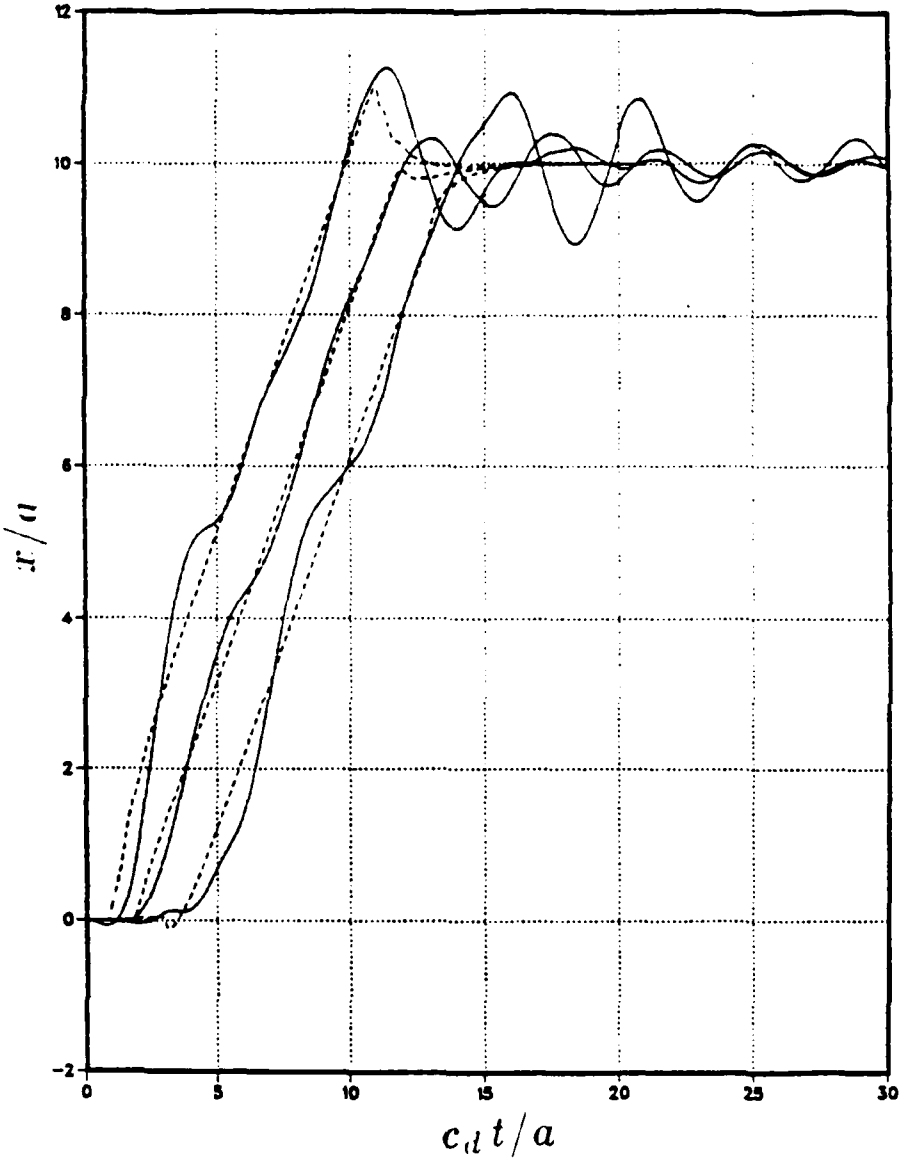


Figure 8. Displacement response histories for spherical shell (solid curves: finite elements around shell: dashed curves: DAA boundary on shell surface).

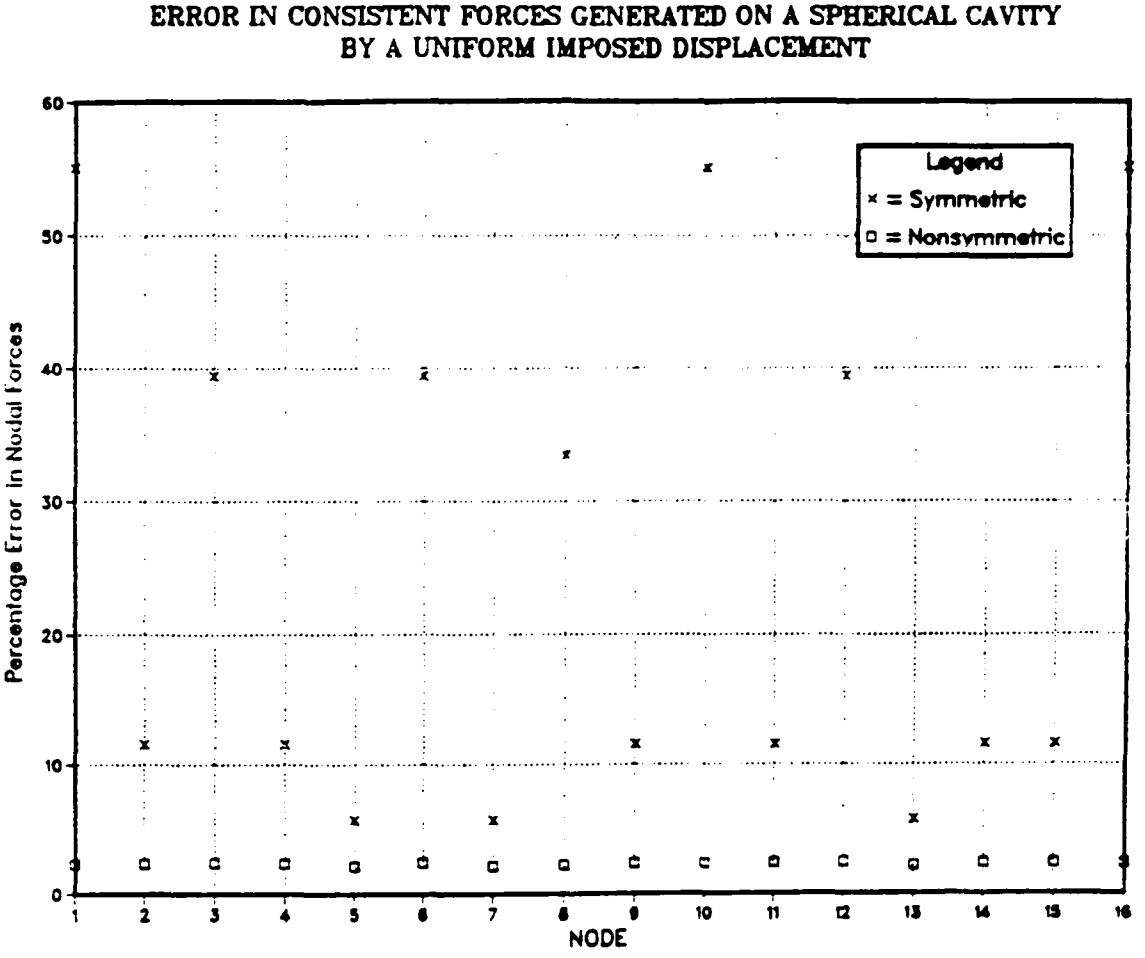


Figure 9. Error in nodal-force values produced by symmetric and nonsymmetric medium stiffness matrices.

# APPENDIX A

# NUMERICAL INTEGRATION TECHNIQUES

Discretization of the DAA boundary makes it possible to approximate (3.1) by a system of linear algebraic equations for nodal values of surface displacement and traction, *i.e.*, (3.14). The coefficients in these equations are obtained by integrating, by means of quadrature formulas, products of kernel functions and shape functions over the boundary elements, as indicated in (3.13). In this regard, it is necessary to distinguish between to fundamentally different types of integrals that arise.

The first type of integral occurs when the node P *does not belong* to the element over which the integral is being performed. This type is *regular*, because the integrand varies smoothly over the surface. Simple Gaussian quadrature formulas may then be used. In two dimensions,

$$\int_{-1}^{+1} f(\xi)\, d\xi \approx \sum_{l=1}^{M} w_l\, f(\xi_l) \tag{A.1}$$

where the $w_l$ are weighting factors, the $\xi_l$ are the coordinates of the integration points and $M$ is the total number of integration points. Similarly, in three dimensions,

$$\int_{-1}^{+1}\int_{-1}^{+1} f(\xi_1, \xi_2)\, d\xi_1 d\xi_2 \approx \sum_{l=1}^{M}\sum_{m=1}^{M} w_l\, w_m\, f(\xi_{1l}, \xi_{2m}) \tag{A.2}$$

The second type of integral occurs when the node P *belongs* to the element over which the integral is being performed. This type is *singular*, because the integrand grows without bound at P. The techniques used to evaluate the singular integrals encountered in this study are described below.

## A.1 Singular Integrals Involving the Traction Kernel

For this singular case, there exists no quadrature formula suitable for the calculation of the integral $T_{ij}$. The coefficient of this integral for the singular node together with the $c_{ij}$ term form the leading diagonal submatrix of coefficients of $u_j$ in equation (3.13). These coefficients can be expediently calculated by noting that a stress field corresponding to a rigid body translation of the body is zero. In this case equation (3.14) becomes

$$\mathbf{A}\,\mathbf{u} = 0 \tag{A.3}$$

where $\mathbf{u}$ is a vector of unit rigid body displacements. The diagonal terms of A are simply given by

$$a_{ii} = 1 - \sum_{i \neq j} a_{ij} \tag{A.4}$$

## A.2 Singular Integrals Involving the Displacement Kernel

In two dimensions, a quadrature rule based on the theory of [*Takahasi and Mori (1973)*] is utilized integrate the $ln(r)$ singularity contained in the $U_{ij}$ kernel. Such a quadrature rule has been successfully used for two-dimensional acoustic scattering problems [*Burton 1976*]. First, let the integration of this singularity in the intrinsic coordinate system be represented by

$$I = \int_{-1}^{1} f(\xi)\, d\xi \tag{A.5}$$

where $f(\xi)$ may have singularities at $\pm 1$. Then the value of this integral is given by the following quadrature formula

$$I \approx \sum_{n=-N}^{N} w_n f(\xi_n) \tag{A.6}$$

where

$$w_n = \frac{2h}{\sqrt{\pi}} e^{-n^2 h^2}$$

$$\xi_n = erf(nh)$$

The values of $N = 4$ and $h = 0.75$ were used to construct a 9-point, one-dimensional quadrature rule. The error in integrating $ln(\xi)$ over $(0, 1)$ with these points is less than $6 \times 10^{-6}$. The method has been shown to be capable to handle singularities of composite or undetermined types [*Burton 1976*]. When the singularity is at the center node of the 3 noded quadratic element, the element is subdivided such that the quadrature rule can be applied on either side of the node.

In three dimensions a technique given by [*Lachat & Watson 1976*] was used to integrate the $1/r$ singularity in $U_{ij}$. The $2 \times 2$ basis square in $\xi_1, \xi_2$ -space on which the non-singular integrals are evaluated is subdivided into triangles, the singular nodes always at the vertex. The triangles are given a new intrinsic coordinate system $(\eta_1, \eta_2)$ obtained by viewing the triangle as a degenerated rectangle in the $(\xi_1, \xi_2)$ space. The relationship between the two sets of intrinsic coordinates is given in terms of linear shape functions defined by

$$\xi_i(\eta) = \sum_{a=1}^{4} N^{(a)}(\eta) \xi_i^{(a)} \tag{A.7}$$

where $N^a(\eta)$ represent the linear shape functions. These triangular subelements in the $(\eta_1, \eta_2)$ space form a Jacobian that has $0(r)$ behaviour. The $0(1/r)$ singularity of the kernel is removed numerically when multiplied by this Jacobian with $0(r)$ behaviour.

## A.3 Geometrical Symmetry

Symmetry of the DAA boundary with respect to coordinate axes is accounted for within the software. This is implemented by reflecting each element about the symmetry axis during the construction of the $A$ and $B$ matrices (equation 3.14). Care however, is required,when using the *rigid body* methodology to calculate the diagonal terms of the traction kernel $T_{ij}$. in that the summation of the off-diagonal terms must be performed before the symmetry transformation is applied to each component of $T_{ij}$. Also, the displacements and tractions at the nodes on the plane of symmetry in the direction across the plane must be eliminated because they are zero. This is done by zeroing the corresponding rows and columns and by placing the value 1.0 on the leading diagonal.

# APPENDIX B

## SYMMETRIC AND NONSYMMETRIC MEDIUM STIFFNESS MATRICES

The accuracy of symmetric and nonsymmetric medium stiffness matrices is evaluated here by computing the nodal forces generated by a uniform displacement field applied to a spherical cavity in an infinite elastic medium. The correct nodal forces follow from the known traction solution [*Timoshenko and Goodier 1951*] and (3.16), the nodal forces produced by the nonsymmetric stiffness matrix follow from (3.17), and the nodal forces produced by the symmetric stiffness matrix follow from (3.17) with $\mathbf{K}_m$ replaced by $\hat{\mathbf{K}}_m$. Figure 9 shows, for the discretization of Figure 5, computational error in nodal-force magnitudes computed with the symmetric and nonsymmetric matrices: $\mathbf{K}_m$ clearly outperforms $\hat{\mathbf{K}}_m$. It should be noted, that convergence of the nodal forces generated by the symmetric medium matrix $\hat{\mathbf{K}}_m$ was obtained by successive mesh refinement.

# DISTRIBUTION LIST

**DEPARTMENT OF DEFENSE**

ASSISTANT TO THE SECRETARY OF DEFENSE
ATOMIC ENERGY
ATTN: EXECUTIVE ASSISTANT

DEFENSE ADVANCED RSCH PROJ AGENCY
ATTN: T BACHE

DEFENSE INTELLIGENCE AGENCY
ATTN: DB-4C
ATTN: RTS-2B
ATTN: VP-TPO

DEFENSE NUCLEAR AGENCY
2 CYS ATTN: SPAS G ULLRICH
4 CYS ATTN: STTI-CA

DEFENSE TECHNICAL INFORMATION CENTER
12 CYS ATTN: DD

FIELD COMMAND DNA DET 2
LAWRENCE LIVERMORE NATIONAL LAB
ATTN: FC-1

FIELD COMMAND DEFENSE NUCLEAR AGENCY
ATTN: FCPR
ATTN: FCTK C KELLER
ATTN: FCTT
ATTN: FCTT W SUMMA
ATTN: FCTXE

JOINT STRAT TGT PLANNING STAFF
ATTN: JLK (ATTN: DNA REP)
ATTN: JLKS
ATTN: JPST
ATTN: JPTM

UNDER SECYS OF DEF FOR RSCH & ENGRG
ATTN: STRAT & SPACE SYS(OS)
ATTN: STRAT & THEATER NUC FOR F VAJDA

**DEPARTMENT OF THE ARMY**

BMD ADVANCED TECHNOLOGY CENTER
ATTN: ATC-T
ATTN: ICRDAHB-X

HARRY DIAMOND LABORATORIES
ATTN: DELHD-TA-L (81100)(TECH LIB)
ATTN: SCHLD-NW-P

U S ARMY BALLISTIC RESEARCH LAB
ATTN: SLCBR-SS-T (TECH LIB)

U S ARMY CONCEPTS ANALYSIS AGENCY
ATTN: CSSA-ADL (TECH LIB)

U S ARMY CORPS OF ENGINEERS
ATTN: DAEN-ECE-T
ATTN: DAEN-RDL

U S ARMY ENGINEER CTR & FT BELVOIR
ATTN: DT-LRC

U S ARMY ENGINEER DIV HUNTSVILLE
ATTN: HNDED-SR

U S ARMY ENGINEER DIV OHIO RIVER
ATTN: ORDAS-L (TECH LIB)

U S ARMY ENGR WATERWAYS EXPER STATION
ATTN: J STRANGE
ATTN: J ZELASKO
ATTN: LIBRARY
2 CYS ATTN: WESSD J JACKSON
ATTN: WESSE

U S ARMY MATERIAL COMMAND
ATTN: DRXAM-TL (TECH LIB)

U S ARMY MATERIAL TECHNOLOGY LABORATORY
ATTN: TECHNICAL LIBRARY

U S ARMY NUCLEAR & CHEMICAL AGENCY
ATTN: LIBRARY

USA MISSILE COMMAND
ATTN: DOCUMENTS SECTION

**DEPARTMENT OF THE NAVY**

LEAHY (CG 16)
ATTN: WEAPONS OFFICER

NAVAL FACILITIES ENGINEERING COMMAND
ATTN: CODE 04B

NAVAL POSTGRADUATE SCHOOL
ATTN: CODE 1424 LIBRARY

NAVAL RESEARCH LABORATORY
ATTN: CODE 2627 (TECH LIB)

NAVAL SURFACE WEAPONS CENTER
ATTN: CODE F31

NAVAL SURFACE WEAPONS CENTER
ATTN: TECH LIBRARY & INFO SVCS BR

NAVAL UNDERWATER SYSTEMS CTR
ATTN: CODE EM J KALINOWSKI

**DEPARTMENT OF THE NAVY (CONTINUED)**

NAVAL WAR COLLEGE
ATTN: CODE E-11 (TECH SERVICE)

NAVAL WEAPONS EVALUATION FACILITY
ATTN: CLASSIFIED LIBRARY

OFC OF THE DEPUTY CHIEF OF NAVAL OPS
ATTN: NOP 03EG
ATTN: NOP 981

OFFICE OF NAVAL RESEARCH
ATTN: CODE 474 N PERRONE

SPACE & NAVAL WARFARE SYSTEMS CMD
ATTN: PME 117-21

STRATEGIC SYSTEMS PROGRAMS (PM-1)
ATTN: NSP-43 (TECH LIB)

**DEPARTMENT OF THE AIR FORCE**

AFIS/INT
ATTN: INT

AIR FORCE GEOPHYSICS LABORATORY
ATTN: LWH/H OSSING

AIR FORCE INSTITUTE OF TECHNOLOGY
ATTN: LIBRARY

AIR FORCE OFFICE OF SCIENTIFIC RSCH
ATTN: J ALLEN
ATTN: W BEST

AIR FORCE SYSTEMS COMMAND
ATTN: DLW

AIR FORCE WEAPONS LABORATORY, AFSC
ATTN: NTE M PLAMONDON
ATTN: NTED J THOMAS
ATTN: NTED R HENNY
ATTN: SUL

AIR UNIVERSITY LIBRARY
ATTN: AUL-LSE

BALLISTIC MISSILE OFFICE/DAA
ATTN: EN
ATTN: MGEN A SCHENKER
ATTN: MGEN E FURBEE
ATTN: PP

DEPUTY CHIEF OF STAFF
ATTN: LEEE

DEPUTY CHIEF OF STAFF/AF-RDQI
ATTN: AF/RDQI

FOREIGN TECHNOLOGY DIVISION, AFSC
ATTN: NIIS LIBRARY

ROME AIR DEVELOPMENT CENTER, AFSC
ATTN: TSLD

STRATEGIC AIR COMMAND
ATTN: INA

STRATEGIC AIR COMMAND
ATTN: NRI/STINFO

STRATEGIC AIR COMMAND
ATTN: XPFS

STRATEGIC AIR COMMAND
ATTN: XPQ

**DEPARTMENT OF ENERGY**

DEPARTMENT OF ENERGY
ALBUQUERQUE OPERATIONS OFFICE
ATTN: CTID
ATTN: R JONES

DEPARTMENT OF ENERGY
NEVADA OPERATIONS OFFICE
ATTN: DOC CON FOR TECHNICAL LIBRARY

LAWRENCE LIVERMORE NATIONAL LAB
ATTN: L-221 D GLENN
ATTN: L-53 TECH INFO DEPT LIBRARY

LOS ALAMOS NATIONAL LABORATORY
ATTN: MS P364 REPORTS LIBRARY

OAK RIDGE NATIONAL LABORATORY
ATTN: CENTRAL RSCH LIBRARY
ATTN: CIVIL DEF RES PROJ

SANDIA NATIONAL LABORATORIES
ATTN: LIBRARY & SECURITY CLASSIFICATION DIV

SANDIA NATIONAL LABORATORIES
ATTN: ORG 7111 L HILL
ATTN: ORG 7112 A CHABAI
ATTN: TECH LIB 3141

**OTHER GOVERNMENT**

CENTRAL INTELLIGENCE AGENCY
ATTN: OSWR/NED

DEPARTMENT OF THE INTERIOR
ATTN: TECH LIB

**DEPARTMENT OF DEFENSE CONTRACTORS**

AEROSPACE CORP
ATTN: LIBRARY ACQUISITION M1/199

APPLIED RESEARCH ASSOCIATES, INC
ATTN: N HIGGINS

APPLIED RESEARCH ASSOCIATES, INC
ATTN: S BLOUIN

APPLIED RESEARCH ASSOCIATES, INC
ATTN: D PIEPENBURG

APPLIED RESEARCH ASSOCIATES, INC
ATTN: R FRANK

AVCO SYSTEMS DIVISION
ATTN: LIBRARY A830

BDM CORP
ATTN: A VITELLO
ATTN: CORPORATE LIB

**DEPT OF DEFENSE CONTRACTORS (CONTINUED)**

BDM CORP
ATTN: F LEECH

BOEING CO
ATTN: M/S 8K-22 D CHOATE

CALIFORNIA INSTITUTE OF TECHNOLOGY
ATTN: T AHRENS

CALIFORNIA RESEARCH & TECHNOLOGY, INC
ATTN: K KREYENHAGEN
ATTN: LIBRARY
ATTN: M ROSENBLATT
ATTN: S SCHUSTER

CALIFORNIA RESEARCH & TECHNOLOGY, INC
ATTN: F SAUER

CALSPAN CORP
ATTN: LIBRARY

CARPENTER RESEARCH CORP
ATTN: H J CARPENTER

UNIVERSITY OF DENVER
ATTN: J WISOTSKI

IIT RESEARCH INSTITUTE
ATTN: DOCUMENTS LIBRARY
ATTN: M JOHNSON

INSTITUTE FOR DEFENSE ANALYSES
ATTN: CLASSIFIED LIBRARY

KAMAN SCIENCES CORP
ATTN: L MENTE
ATTN: LIBRARY

KAMAN SCIENCES CORP
ATTN: LIBRARY

KAMAN TEMPO
ATTN: DASIAC

KAMAN TEMPO
ATTN: DASIAC

LOCKHEED MISSILES & SPACE CO, INC
2 CYS ATTN: I MATHEWS
ATTN: J BONIN
2 CYS ATTN: T GEERS

LOCKHEED MISSILES & SPACE CO, INC
ATTN: J WEISNER

MAXWELL LABORATORIES, INC
ATTN: J MURPHY

MCDONNELL DOUGLAS CORP
ATTN: R HALPRIN

MERRITT CASES, INC
ATTN: J MERRITT
ATTN: LIBRARY

NEW MEXICO ENGINEERING RESEARCH INSTITUTE
ATTN: N BAUM

PACIFIC-SIERRA RESEARCH CORP
ATTN: H BRODE, CHAIRMAN SAGE

PATEL ENTERPRISES, INC
ATTN: M PATEL

R & D ASSOCIATES
ATTN: C K B LEE
ATTN: D SIMONS
ATTN: J LEWIS
ATTN: P HAAS
ATTN: TECHNICAL INFORMATION CENTER
ATTN: W WRIGHT

R & D ASSOCIATES
ATTN: G GANONG

RAND CORP
ATTN: P DAVIS

RAND CORP
ATTN: B BENNETT

S-CUBED
ATTN: D GRINE
ATTN: LIBRARY
ATTN: T RINEY

SCIENCE APPLICATIONS INTL CORP
ATTN: TECHNICAL LIBRARY

SCIENCE APPLICATIONS INTL CORP
ATTN: D MAXWELL

SCIENCE APPLICATIONS INTL CORP
ATTN: W LAYSON

SOUTHWEST RESEARCH INSTITUTE
ATTN: A WENZEL

SRI INTERNATIONAL
ATTN: D KEOUGH

STRUCTURAL MECHANICS ASSOC, INC
ATTN: R KENNEDY

TELEDYNE BROWN ENGINEERING
ATTN: D ORMOND
ATTN: F LEOPARD

TERRA TEK, INC
ATTN: S GREEN

TRW ELECTRONICS & DEFENSE SECTOR
2 CYS ATTN: N LIPNER
ATTN: P BHUTA
ATTN: TECHNICAL INFORMATION CENTER

TRW ELECTRONICS & DEFENSE SECTOR
ATTN: E WONG
ATTN: P DAI

WEIDLINGER ASSOC, CONSULTING ENGRG
ATTN: T DEEVY

WEIDLINGER ASSOC, CONSULTING ENGRG
ATTN: M BARON

WEIDLINGER ASSOC, CONSULTING ENGRG
ATTN: J ISENBERG

END

DTIC

7-86